Title: Otolith increments in common sole (*Solea solea*) reveal fish growth plasticity to temperature

Author names (given name + **last name**):

Tuan Anh **Bui**[1,2], Marleen **De Troch**[1], Jan Jaap **Poos**[3,4], Adriaan **Rijnsdorp**[4], Bruno **Ernande**[5], Karen **Bekaert**[2], Kélig **Mahé**[6], Kelly **Díaz**[1], Jochen **Depestele**[2]

Affiliations:

[1]Ghent University, Department of Biology, Marine Biology Research Group, Krijgslaan 281/S8, Ghent, Belgium

[2]Flanders Research Institute for Agriculture, Fisheries and Food (ILVO), Oostende, Belgium

[3]Aquaculture and Fisheries Group, Wageningen University and Research, Wageningen, The Netherlands

[4]Wageningen Marine Research, Wageningen University and Research, IJmuiden, The Netherlands

[5]MARBEC, Univ. Montpellier, Ifremer, CNRS, IRD, Montpellier, France

[6]IFREMER, Unité HMMN, 150 quai Gambetta, 62321 Boulogne-sur-Mer, France

Corresponding author: Tuan Anh Bui; tuananh.bui@ugent.be; Ghent University, Department of Biology, Marine Biology Research Group, Krijgslaan 281/S8, 9000 Ghent, Belgium.

Abstract

Phenotypic plasticity is a major mechanism allowing organisms to respond to environmental variability. Understanding phenotypic plasticity of organisms to warming is crucial to predict future impacts of climate change. In this study, we investigated fish growth plasticity to temperature using a large archive of otoliths collected from 1960 to 2020, providing growth data over the period 1958-2019, of three common sole (*Solea solea*) populations: North Sea, Irish Sea, and Bay of Biscay. We used mixed-effects models to partition growth variation into its intrinsic (age, age at capture) and extrinsic (temperature, density, fishing pressure, nutrient) components; to disentangle individual-level plasticity from the population-level response to temperature; and to assess the environmental dependency of growth plasticity. We demonstrated that sole growth plasticity followed the Temperature-Size Rule with increasing juvenile growth and decreasing adult growth at higher temperature. Under favourable conditions for sole growth, the positive response to warming in juvenile fish is stronger while the negative response in adult fish is weaker and the individual plasticity variance is lower. Our study provides additional support for the universality of the Temperature-Size Rule and contributes to our understanding of fish populations' responses to current and future climate change.

Keywords: Temperature-Size Rule, plasticity, *Solea solea*, otolith, growth, life history

1 Introduction

Global warming is accelerating rapidly (IPCC, 2021), raising concerns on the responses of organisms. Fish, ectothermic organism whose body temperature depend on ambient temperature, are especially sensitive to warming (Pinsky et al., 2019). Changes in distribution (Baudron et al., 2020; Poloczanska et al., 2016; Rutterford et al., 2015) and phenology (Neuheimer et al., 2018; Poloczanska et al., 2016) have been well documented as universal responses of fish to warming. An increasing number of studies has focused on the response to warming of somatic growth, given its importance to individual fitness and population metrics such as reproductive output and stock biomass (Hixon et al., 2014; Stawitz and Essington, 2019). Field and experimental studies have shown that fish living in warmer temperatures grow faster but reach a smaller maximum size (Atkinson, 1994; Baudron et al., 2014; Ikpewe et al., 2021; Smoliński et al., 2020a; van Rijn et al., 2017; Wang et al., 2020; Wootton et al., 2022). This response is referred to as the Temperature-Size Rule (TSR) (Atkinson,

1994). However, the generality of TSR-type response remains debated, because several studies found contrasting results to TSR such as larger maximum size at warmer temperature (Audzijonyte et al., 2020; Lindmark et al., 2023; Mollet et al., 2013).

The TSR deals with growth plasticity to temperature (Atkinson, 1994), which refers to the variation of growth of the same individual when experiencing temperature variation within its lifetime. An individual with positive plasticity grows faster in warmer years but slower in cooler years. Plasticity is at individual level and cannot always possibly be inferred in field studies from the population-level response (correlation between the mean population growth rate and temperature) (Morrongiello et al., 2019; Smoliński et al., 2020a; van de Pol and Wright, 2009). This is due to the confounding between-individual effects, which refers to the variation of growth across different individuals due to genetic and/or environmental differences; e.g. individuals living in the warmer period having higher growth than those living in cooler period might be because of more food availability associated with warming. Disentangling plasticity from the population-level response is important to assess the TSR.

Another important question is how growth plasticity to temperature is influenced by environmental conditions, because this can contribute to our capacity to predict how fish populations respond to environmental changes. Answering this question requires the assessment of the environmental dependency of growth plasticity both in terms of plasticity magnitude (i.e. whether the average plasticity of individuals in the population increases or decreases with environmental changes) and in terms of individual plasticity variance (i.e. whether the individual-specific plasticity of individuals in the population is more homogenous or more heterogenous with environmental changes). The latter is an element of biocomplexity, which reflects the resilience of a population to environmental change (Hilborn et al., 2003; Schindler et al., 2010). The environmental dependency of plasticity magnitude and of individual plasticity variance remain largely unexplored despite many studies on growth-temperature relationships in fish (Morrongiello et al., 2021; Morrongiello et al., 2019; Smoliński et al., 2020a). Potential factors affecting growth, and thus the environmental dependency of growth plasticity, include density and fishing pressure (Denechaud et al., 2020; Morrongiello et al., 2021; van der Sleen et al., 2018). Density can influence growth through intraspecific competition for food (Lorenzen and Enberg, 2002); while fishing removes a proportion of individuals (usually larger and older) from populations and can influence growth through genetic

selection of fast- or slow-growing individuals (fisheries induced evolution) (Enberg et al., 2012; Heino et al., 2015; Lee, 1912) and/or release from density dependence (Planque et al., 2010).

In this paper, we aim to investigate (1) fish growth plasticity to temperature; and (2) the environmental dependency of growth plasticity, both in terms of plasticity magnitude and individual plasticity variance. We used otolith data. Otoliths are calcified structures in the inner ear of fish and otolith rings, like tree rings, are often formed annually (Black et al., 2005; Millner and Whiting, 1996; Vitale et al., 2019). The periodic deposition of otolith rings reflects the growth trajectory as well as the changes in intrinsic (e.g. age) and extrinsic (e.g. temperature) factors throughout a fish's life (Campana and Thorrold, 2001; Morrongiello et al., 2012). Therefore, otolith data offer a unique opportunity to study growth plasticity to temperature and its dependency on environmental changes.

We selected common sole *(Solea solea)* as a case-study species because it has a long exploitation history (Engelhard et al., 2011; Lescrauwaet et al., 2010; Rijnsdorp and Van Beek, 1991), and biological data, including otoliths, have been collected for many decades as part of fisheries management in Europe (ICES, 2020). Sole is a warm-favouring and bottom-dwelling flatfish species that is widely distributed across North-East Atlantic, ranging from the North Sea in the north to the northwest African coast in the south (Lefrancois and Claireaux, 2003; OBIS, 2023; Schram et al., 2013). It matures at age 2-3, can live more than 25 years, and can reach a maximum length of 70 cm (Mollet et al., 2013; Mollet et al., 2007). Juvenile soles are often more abundant in coastal areas while adult soles prefer deeper waters (Rijnsdorp and Van Beek, 1991; Rijnsdorp et al., 1992). The opaque zone of sole otolith usually forms in May-October and the translucent zone usually forms in November-April (Amara, 2003; Millner and Whiting, 1996). Sole is a major target of beam trawl fisheries (Engelhard et al., 2011; Lescrauwaet et al., 2010), with a minimum conservation reference size (formerly known as minimum landing size) of 24 cm (EC, 2019). We collected sole otoliths from the North Sea, the Irish Sea, and the Bay of Biscay populations (Figure 1A). These populations have experienced rapid warming rates above the global average (Garcia-Soto et al., 2021; Tinker and Howes, 2020), and variable density level and fishing pressure (ICES, 2023a, b, c) (Figure 1B-E).

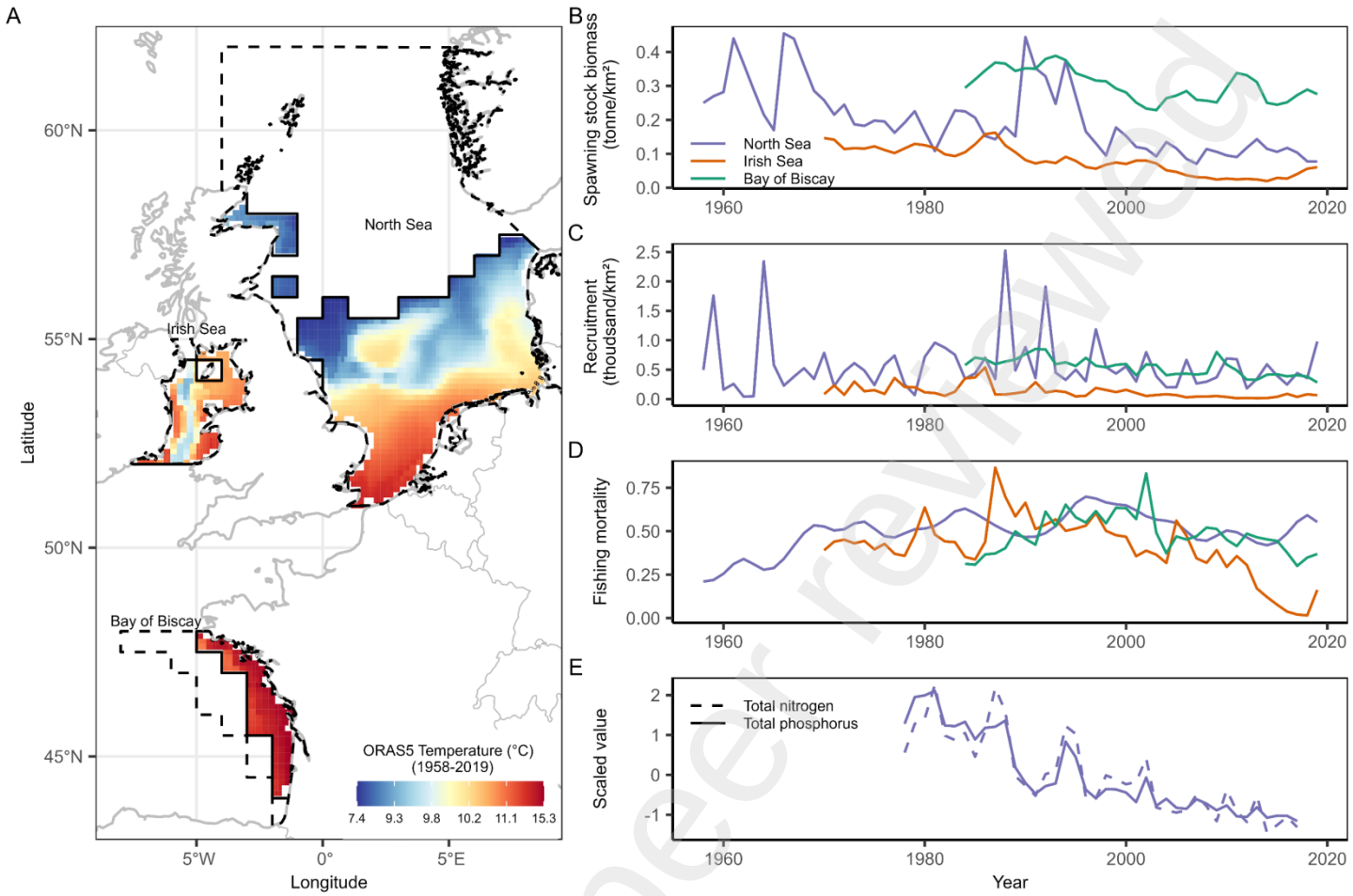

Figure 1. Map of the study area (A) with indications of stock management areas (dashed line), distribution areas of sole estimated from beam trawl survey data (solid line), and average annual bottom temperature over the 1958-2019 period from ORAS5 (Ocean Reanalysis System 5) data (Copernicus Climate Change Service, 2021) (see Materials and methods); Temporal trend of spawning stock biomass, recruitment, fishing mortality, and nutrient concentrations (total nitrogen, total phosphorus) in the study area (B-E).

2 Materials and methods

2.1 Otolith data

Otoliths from female sole were sampled from archives at the Flanders Research Institute for Agriculture, Fisheries, and Food (ILVO), Wageningen University & Research (WUR), and the French Research Institute for Exploitation of the Sea (IFREMER) (Table 1). ILVO otoliths collected before the year 2000 were prepared using broken-and-burned method (Vitale et al., 2019): otoliths were broken transversally in half (as close to the nucleus as possible) and were then burned until

the translucent rings became grey and more visible (Figure S1). ILVO otoliths collected from the year 2000 onwards and WUR otoliths were prepared using sectioned-and-stained method (Vitale et al., 2019): otoliths were embedded in resin and sectioned transversally through the nucleus into 0.5-0.6 mm thin slices and were then stained with alizarin red to make the translucent ring more visible (Figure S2, Figure S3, and Figure S4). IFREMER otoliths were transversally sectioned without staining (Figure S5).

Archive	Population	Number of otoliths	Collection period	Preparation method	Reading institute
ILVO	North Sea	720	1973-2020	Broken-and-burned (before 2000) Sectioned-and- stained (since 2000)	ILVO
	Irish Sea	761			
	Bay of Biscay	204			
WUR	North Sea	431	1960-2001	Sectioned-and-stained	WUR
IFREMER	Bay of Biscay	40	2012-2017	Sectioned	ILVO

Table 1. Summary of otolith sampling. The reading institute indicates the institute that was responsible for reading the otolith increments.

We used the stratified sampling approach, i.e., multiple cohorts were sampled over time and each cohort included multiple fish of different ages at capture, ranging from 3 to 25 years (Figure S6) (Morrongiello et al., 2012). We sampled three otoliths per age class wherever possible. To minimise bias in growth estimation, we selected only otoliths with clearly visible nucleus and rings; and only broken-and-burned otoliths with a relatively flat broken surface. In total, 2156 otoliths were sampled (Table 1, Figure S6, Figure S7).

Sampled otoliths were photographed using a high-resolution digital camera connected to a stereomicroscope. For each otolith, the width of each growth ring was measured along a single growth axis (**Error! Reference source not found.**) (Bolle et al., 2004). This width-measuring approach, compared to the conventional radius-measuring approach, overcomes the possible bias caused by differences in growth pattern in both sides of sole otoliths (Rijnsdorp et al., 1990). Measurements of WUR otoliths were extracted from WUR's historical database (Mollet, 2010). ILVO and IFREMER otoliths were measured

at ILVO using SmartDots software (http://smartdots.ices.dk). Aging precision of 99.5% of newly read otoliths was tested and confirmed through re-aging by an experienced expert at ILVO (CV < 3%, see Table S1).

We used otolith increment, i.e. the width difference between subsequent rings, as a proxy of somatic growth as fish length is correlated with otolith width (R^2 = 0.53; see Figure S8) . In subsequent analyses, years with less than 10 increment measurements were excluded. In total, 2154 otoliths with 15260 increments formed in the 1958-2019 period were analysed.

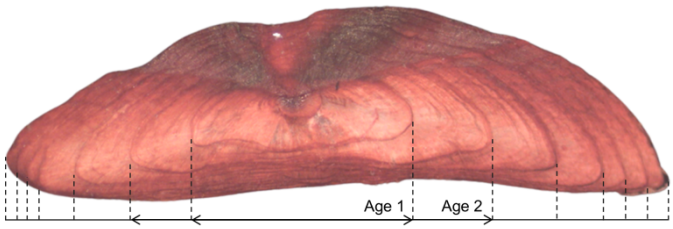

Figure 2. Common sole otolith after being transversally sectioned and stained. The width of each growth ring was measured along a single growth axis.

2.2 Predictors of fish growth

We selected a series of potential intrinsic and extrinsic predictors of sole growth (**Error! Reference source not found.**). Intrinsic predictors include age and age at capture. Age at capture was used to account for potential growth difference between younger and older fish caused by fishing selectivity (Lee, 1912; Morrongiello and Thresher, 2015). Preparation method and reading institute were included to control for the potential difference in measurements among preparation methods and reading institutes.

Extrinsic predictors include temperature, spawning stock biomass, recruitment, fishing mortality, and nutrients. We used modelled bottom temperature from three datasets: ISIMIP (Inter-Sectoral Impact Model Intercomparison Project) simulation round 3b (code mpi-esm1-2-hr_r1i1p1f1_<climate-scenario>_tob) (Büchner, 2020), ORAS5 (Ocean Reanalysis System 5) (Copernicus Climate Change Service, 2021), and NEMO-MEDUSA (Nucleus for European Modelling of the Ocean - Model of Ecosystem Dynamics, nutrient Utilization, Sequestration and Acidification) (Yool et al., 2013; Yool et al., 2015). ISIMIP and ORAS5 data were available over the study period (1958-2019) while NEMO-MEDUSA data were only available from 1980 onwards. Spatial resolution ranged from 0.25° for ORAS5 and NEMO-MEDUSA to 1° for ISIMIP. We used ISIMIP

SSP5-8.5 data to be comparable with NEMO-MEDUSA RCP 8.5 data. All datasets were well correlated with *in situ* bottom temperature records from the International Council for the Exploration of the Sea (ICES) High Resolution CTD data (1970-2021) (ICES, 2022) - North Sea: R^2 = 0.87-0.96, Irish Sea: R^2 = 0.76-0.93, Bay of Biscay: R^2 = 0.31-0.54 (Appendix S2, Table S2).

Temperature was averaged by year over the distribution areas of sole (Table S11). These distribution areas were estimated from beam trawl survey data (1985-2022) (DATRAS, 2023) (Figure 1A, Appendix S3). We used annual temperatures because otolith growth, despite usually being maximal in summer and minimal in winter (Amara, 2003; Millner and Whiting, 1996), occurs year-round and there might be difference in deposition timing among life stages or individuals (Kimura et al., 2007; Millner and Whiting, 1996; Vitale et al., 2019). In addition, annual mean temperatures were well correlated with seasonal mean temperatures, with R^2 ranging from 0.51 in autumn to 0.96 in summer (Table S3).

Spawning stock biomass and recruitment were used to test for the effect of density on the growth of adult and juvenile sole, respectively. Spawning stock biomass and recruitment were divided by the distribution areas estimated from survey data (Figure 1A, Appendix S3) to standardise the differences in absolute value among the study populations (Figure S14). Fishing mortality was used to test for the effect of fishing pressure on sole growth. Spawning stock biomass, recruitment, and fishing mortality were extracted from the ICES stock assessments (ICES, 2023a, b, c; Millar et al., 2023).

Total nitrogen and total phosphorus were used to test for the effect of nutrients on sole growth. Total nitrogen and total phosphorus estimates (kilotonne/year) were extracted from the OSPAR ICG-EMO riverine database (van Leeuwen and Lenhart, 2021) for the major rivers in the North Sea in the 1978-2017 period. These riverine inputs accounted for more than 70% of the total input in the area (Figure S15).

Predictor	**Description**
Random effects	
FishID	Unique identifier of a fish individual
Population	Fish population (North Sea, Irish Sea, Bay of Biscay)

Year	Year when the otolith increment is formed
Cohort	Year when the fish is born
Fixed effects	
Age	Age of fish when otolith increment is formed
Age at capture	Age of fish when captured
Preparation method	Otolith preparation method (broken-and-burned, sectioned-and-stained, sectioned)
Reading institute	Institute where otoliths were aged and measured (WUR, ILVO)
Temperature	Mean annual bottom-temperature within the distribution areas of sole. Three temperature datasets were used: ISIMIP, ORAS5, NEMO-MEDUSA.
Spawning stock biomass	Total weight of all individuals in a stock that have reached sexual maturity divided by distribution areas (tonne/km^2)
Recruitment	Number of fish at age 1 (North Sea) or 2 (Irish Sea, Bay of Biscay) divided by distribution areas (thousand/km^2)
Fishing mortality	Mean fishing mortality averaged over age 2-6 (North Sea), 4-7 (Irish Sea), and 3-6 (Bay of Biscay)
Nutrient	Total nitrogen and total phosphorus (kilotonne/year) of major rivers in the North Sea.

Table 2. List of predictors of sole growth.

2.3 Statistical analysis

Statistical analyses included three steps. First, we identified the intrinsic drivers and the temporal trends of growth. Second, we partitioned the temporal trends of growth into its extrinsic drivers and disentangled growth plasticity from the population-level response to temperature; we also tested for the environmental dependency of plasticity magnitude

and the variation of plasticity across individuals. Third, we tested for the environmental dependency of individual plasticity variance using the estimates of individual plasticity from step two.

2.3.1 Intrinsic drivers and temporal trends of growth

We developed an intrinsic model to identify the intrinsic drivers and the temporal trends of growth. Otolith increments decrease exponentially with fish age and this pattern is linearised by taking the natural log of both variables. Age at capture (log-transformed), preparation method, and reading institute were added as additional fixed intrinsic effects. The interactions of age and preparation method and reading institute were included to test for relative differences across preparation methods and reading institutes. Random intercepts and random age slope for fish ID, population, year, and cohort (year and cohort are nested within population) were added as random effects. The random effects allowed to account for systematic (higher or lower growth than average) and relative (differences in age-growth relationship) differences among fish individuals, populations, years, and cohorts. The intrinsic model was fitted using this formula:

where ln(growth) and ln(age) are natural log of annual otolith increment and age at formation. $f_{intrinsic}(.)$ represents additional intrinsic fixed effects (ln(age-at-capture), preparation method, reading institute) and their interactions with ln(age). Random effects are presented in parentheses () with two parts separated by a vertical bar |; the left-hand side describes the design matrices (intercept and ln(age) slope) while the right-hand side describes the grouping factors (fishID, population, and year and cohort nested within population).

$$\begin{aligned} \ln(\text{growth}) \sim \text{intercept} + \ln(\text{age}) + f_{intrinsic}(.) + \\ (1 + \ln(\text{age}) \mid \text{fishID}) + (1 + \ln(\text{age}) \mid \text{population}) + (1 + \ln(\text{age}) \mid \text{population:year}) + (1 + \ln(\text{age}) \mid \\ \text{population:cohort}) + \text{error} \end{aligned} \quad (1)$$

We determined the best (most parsimonious) random effect structure by comparing models with different combinations of random effects and a maximal fixed intrinsic structure (ln(age)*preparation-method + ln(age)*reading-institute + ln(age-at-capture)). Then, we determined the best intrinsic effect structure based on comparisons of models with different combinations of fixed intrinsic effects, while keeping the best random effect structure selected in the previous step. After determining the best intrinsic model, we extracted the best linear unbiased predictors (BLUP) of year random effect to visualise the temporal trends of growth.

Model comparison was based on Akaike's information criterion corrected for small sample sizes (AICc) (Burnham and Anderson, 2002). Models with lower AICc were selected and a reduction of AICc > 2 for each additional variable was considered representing an improvement in model fit (Arnold, 2010). Models were fitted with restricted maximum likelihood (REML) when comparing random effect structures and were fitted with maximum likelihood (ML) when comparing fixed effect structures (Zuur 2009). The best intrinsic model was refitted with REML to obtain unbiased parameter estimation (Zuur 2009). All analyses were conducted in R (R Core Team, 2022) version 4.1.2 with R Studio (RStudio Team, 2022). *lme4* package (Bates et al., 2015) was used to develop linear mixed-effects models and *MuMIn* package (Bartoń, 2022) was used to compare fixed effect structures.

2.3.2 Temperature effect: Population-level response vs. plasticity

We developed extrinsic models, extended from the best intrinsic model developed previously, to partition the temporal trends of growth into its extrinsic drivers and disentangle growth plasticity from the population-level response to temperature. Prior to developing the models, the temperature variable was split into different components to test for different effects of temperature at population and individual levels (**Error! Reference source not found.**). First, temperature was decomposed into population-level spatial and temporal components. Population-specific average temperature ($T_{population\text{-}average}$) was used to quantify population-level response to persistent spatial difference of temperature across populations (**Error! Reference source not found.**C-E); population-specific anomaly ($T_{population\text{-}anomaly}$), which was the difference between the annual temperature of a population and its $T_{population\text{-}average}$, was used to quantify population-level response to temporal variation of temperature within populations (**Error! Reference source not found.**F-H) (Campana et al., 2022; Morrongiello and Thresher, 2015; van de Pol and Wright, 2009). $T_{population\text{-}anomaly}$ was then further split into between-individual and within-individual components. Individual-specific mean temperature ($T_{individual\text{-}average}$) was used to quantify between-individual effect associated with genetic and/or environmental difference across individuals (**Error! Reference source not found.**I-K); Individual-specific temperature anomaly ($T_{individual\text{-}anomaly}$), which was the difference between the annual temperature of an individual and its $T_{individual\text{-}average}$, was used to quantify plasticity to temperature variation within individuals' lifetimes (**Error! Reference source not found.**L-N) (Morrongiello et al., 2019; Smoliński et al., 2020a; van de Pol and Wright, 2009).

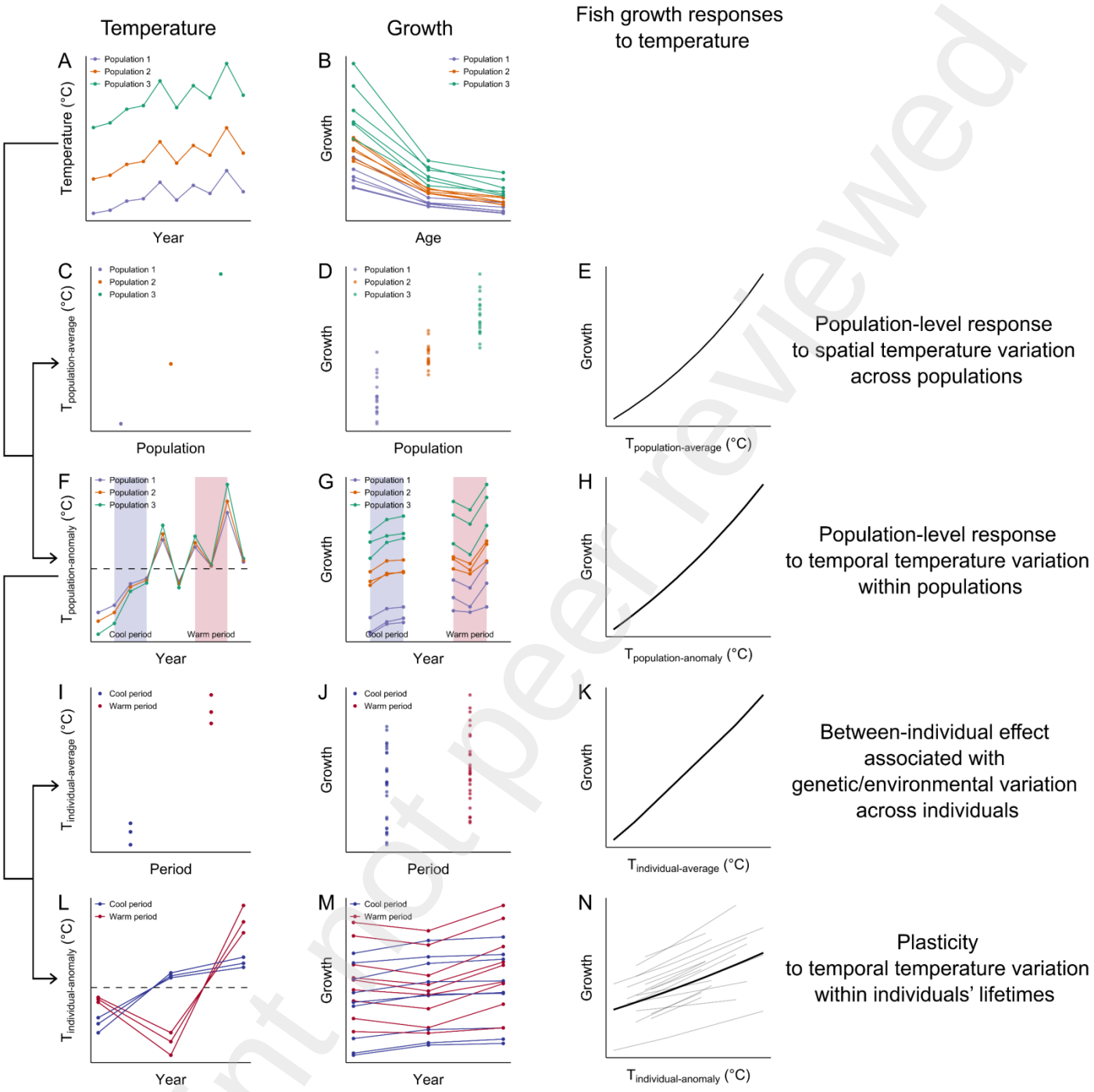

Figure 3. Schematic breakdown of the different temperature components and their corresponding fish growth responses. Absolute temperature (A) can be decomposed into population-level spatial ($T_{population\text{-}average}$ - C) and temporal ($T_{population\text{-}anomaly}$ - F) components, which can be used to quantify population-level response to spatial temperature variation across populations (E) and temporal temperature variation within populations (H). $T_{population\text{-}anomaly}$ can be decomposed into between-individual ($T_{individual\text{-}average}$ - I) and within-individual ($T_{individual\text{-}anomaly}$ - L) components, which can be used to quantify between-individual effect associated with genetic and/or environmental difference across individuals (K) and plasticity to

temperature variation within individuals' lifetimes (N). Note: In (N), the bold line indicates average plasticity and the thin lines indicate individual plasticity. In (F) and (L), the dashed line indicates the population-average and individual-average temperatures. Individual fish are assumed to be collected at age three and in two periods: cool and warm periods when $T_{population\text{-}anomaly}$ is lower and higher than $T_{population\text{-}average}$, respectively (F). Data points in (A) represent growth at age. Data points in (D), (G), (J), and (M) represent residual growth after accounting for age effect, assuming the same age effect across all individuals. Population-level growth responses in (E) and (H) were derived from this model: ln(growth) ~ intercept + ln(age) + $T_{population\text{-}average}$ + $T_{population\text{-}anomaly}$ + (1 | fishID) + error; Between-individual effect (K) and plasticity (N) were derived from this model: ln(growth) ~ intercept + ln(age) + $T_{population\text{-}average}$ + $T_{individual\text{-}average}$ + $T_{individual\text{-}anomaly}$ + (1 + $T_{individual\text{-}anomaly}$ | fishID) + error; where ln(growth) and ln(age) are natural log of growth and age, (1 | fishID) is random intercept for fish ID and (1 + $T_{individual\text{-}anomaly}$ | fishID) is random intercept and random $T_{individual\text{-}anomaly}$ slope for fish ID.

To determine the population-level growth response to temperature, we developed a population-level extrinsic model by adding $T_{population\text{-}average}$ (Figure 3C-E), $T_{population\text{-}anomaly}$ (Figure 3F-H), and other extrinsic effects (i.e., fishing mortality, spawning stock biomass, recruitment) to the best intrinsic model. We included the interactions between $T_{population\text{-}anomaly}$ and age, spawning stock biomass, recruitment, fishing mortality, and $T_{population\text{-}average}$ to test for age- and environment-dependent population-level growth response to temporal variation of temperature. We also included the spawning stock biomass-age and recruitment-age interactions, assuming that the effect of spawning stock biomass is more prevalent for adults while the effect of recruitment is more prevalent for juveniles. We determined the best population-level extrinsic effect structure based on comparisons of models with different combinations of fixed extrinsic effects. Then, we compared models with and without random $T_{population\text{-}anomaly}$ slope for population to test for the variation of population-level growth response to temporal temperature variation across populations. The population-level extrinsic model was fitted using this formula:

$$\begin{aligned} &\ln(\text{growth}) \sim \text{intercept} + \ln(\text{age}) + f_{intrinsic}(.) + \\ &T_{population\text{-}average} + T_{population\text{-}anomaly}*\ln(\text{age}) + T_{population\text{-}anomaly}*T_{population\text{-}average} + f_{extrinsic}(.) + \\ &(1 + \ln(\text{age}) \mid \text{fishID}) + (1 + \ln(\text{age}) + T_{population\text{-}anomaly} \mid \text{population}) + (1 + \ln(\text{age}) \mid \text{population:year}) + \\ &(1 + \ln(\text{age}) \mid \text{population:cohort}) + \text{error} \end{aligned} \quad (2)$$

where an asterisk * represents full interaction terms (main effects and their interaction). $f_{extrinsic}(.)$ represents additional extrinsic fixed effects (fishing mortality, spawning stock biomass, recruitment) and their interactions with $T_{population\text{-}anomaly}$ and ln(age).

To determine the growth plasticity to temperature, we extended the best population-level extrinsic model developed previously into an individual-level extrinsic model by replacing the variable $T_{population\text{-}anomaly}$ with two variables: $T_{individual\text{-}average}$ and $T_{individual\text{-}anomaly}$. This partitioned the population-level growth response to temporal temperature variation into between-individual effect and plasticity (Figure 3F-N) (Morrongiello et al., 2019; Smoliński et al., 2020a; van de Pol and Wright, 2009). We included the interactions between $T_{individual\text{-}anomaly}$ and age, spawning stock biomass, recruitment, fishing mortality, and $T_{individual\text{-}average}$ to test for age- and environment-dependent growth plasticity to temperature. We also included the interaction between $T_{individual\text{-}average}$ and age to test for its age-dependent effect. We determined the best individual-level extrinsic effect structure based on comparisons of models with different combinations of fixed extrinsic effects. Then, we compared models with and without random $T_{individual\text{-}anomaly}$ slope for population and fish ID to test for the variation of plasticity across populations and individuals. The individual-level extrinsic model was fitted using this formula:

$$\begin{aligned} \ln(growth) \sim\ & intercept + \ln(age) + f_{intrinsic}(.) + \\ & T_{individual\text{-}average}*\ln(age) + T_{individual\text{-}anomaly}*\ln(age) + T_{individual\text{-}anomaly}*T_{individual\text{-}average} + f_{extrinsic}(.) + \\ & (1 + \ln(age) + T_{individual\text{-}anomaly} \mid fishID) + (1 + \ln(age) + T_{individual\text{-}anomaly} \mid population) + (1 + \ln(age) \mid \\ & population{:}year) + (1 + \ln(age) \mid population{:}cohort) + error \end{aligned} \quad (3)$$

Model comparison was based on AICc and models were fitted with ML and REML when comparing fixed and random effect structures, respectively (Zuur 2009). The best population-level and individual-level extrinsic models were refitted with REML to obtain unbiased parameter estimation (Zuur 2009), and then refitted with scaled numeric variables (mean zero and standard deviation one) to compare the relative effects of growth predictors. All procedures in developing population-level and individual-level extrinsic models were repeated for each temperature dataset.

After determining the best population-level and individual-level extrinsic models, we refitted the best population-level and individual-level extrinsic models using North Sea data in the 1978-2017 period and added either total nitrogen or

total phosphorus to test for the effect of nutrients on growth. In addition, we refitted the best population-level extrinsic models using data subsets for each population to test if the estimates of density effect (direction, magnitude) differ between the analyses with (full data) and without standardisation (subset data).

2.3.3 Variance of individual plasticity

We compared variance of individual plasticity (random $T_{individual\text{-}anomaly}$ slope for fish ID extracted from the best individual-level extrinsic model) across populations and across cohort-specific mean environmental conditions to test for the environmental dependency of individual plasticity variance. First, we estimated the variance ratio for each pair of population (North Sea/Bay of Biscay, Irish Sea/Bay of Biscay, North Sea/Irish Sea). Given that the range of increment measurements differed across populations (2-21 in the Irish Sea, 2-22 in the North Sea, and 2-11 in the Bay of Biscay with only one fish with 14 measurements) and that the estimated value of individual plasticity may shrink closer to the average plasticity for fish with few measurements, we did the test for different sets of increment measurement ranges: 2-11, 6-11, 2-22, and 6-22 (Morrongiello et al., 2019). In each set, the population with higher sample size was subsampled randomly 100 times to have the same sample size as the other population; then for each subsampling time variance ratio test was conducted using 10,000 bootstrapped samples (Morrongiello et al., 2019). Second, for each population, we did a correlation test between cohort-specific variance of individual plasticity and mean environmental conditions experienced by the cohort ($T_{population\text{-}anomaly}$, fishing mortality, spawning stock biomass, recruitment). The test was done for two sets of increment measurement range: full range and at least six measurements, and only for cohorts with more than five individuals (Morrongiello et al., 2019; Smoliński et al., 2020a).

3 Results

3.1 Intrinsic drivers and temporal trends of growth

The best intrinsic model included age, age at capture, the interaction between age and reading institute, random intercept for fish ID and population, and random intercept and age slope for year (**Error! Reference source not found.**, Table S4, Table S5). The most important driver of growth was age with the strongest growth occurring in age one then decreasing exponentially as age increased (**Error! Reference source not found.**A). There was an effect of age at capture as fish caught at older ages expressed slower growth than fish caught at younger ages (**Error! Reference source not found.**B).

Specifically, a fish caught at age 10 was predicted having annual growth 16.7% slower than a fish caught at age 3. The reading processes also influenced the observed growth pattern. Readings conducted at WUR resulted in larger increments at age 1 (8.6%) and age 2 (0.7%) but smaller increments at older ages (3.6-22.5%), compared to readings conducted at ILVO (Figure S16).

The random structure of the intrinsic model indicated variation of growth among fish individuals, populations, and years. Average growth in the Irish Sea and in the Bay of Biscay was 1.9% higher and 0.2% lower than in the North Sea, respectively (Figure S17). In all populations, juvenile growth (represented by age 1) showed an increasing trend, while adult growth (represented by age 5) showed a decreasing trend (**Error! Reference source not found.**). The trends were clearer in the Irish Sea and in the recent 20 years. For instance, age-1 growth in 2018 was predicted to be 12.1%, 21.2%, and 16.1% faster than in 2000 in the North Sea, the Irish Sea, and the Bay of Biscay, respectively; while age-5 growth in 2018 was predicted to be 5.3%, 15.6%, and 25.3% slower.

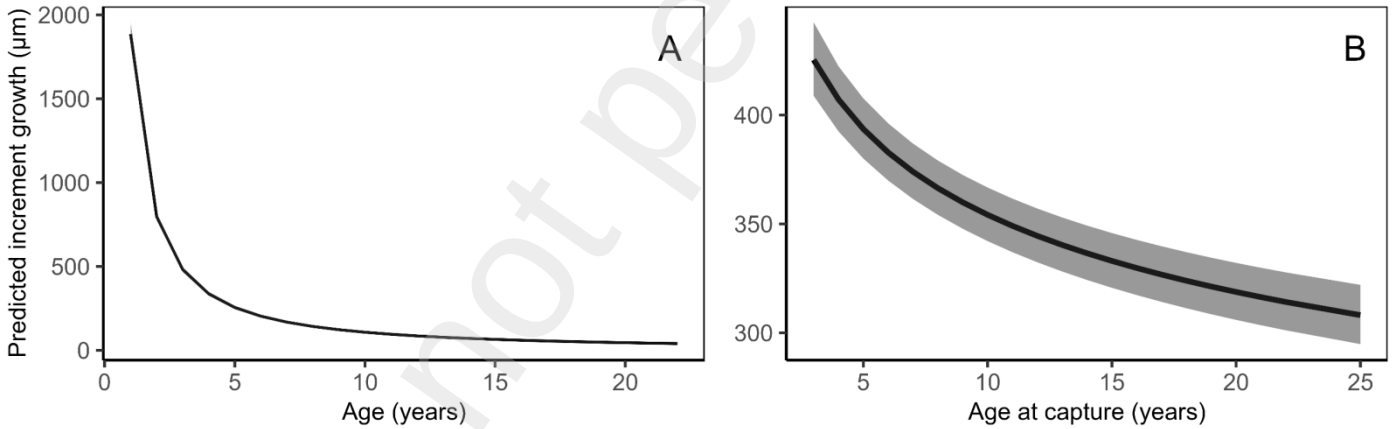

Figure 4. Predicted effect of age (A) and age at capture (B) on sole growth from the best intrinsic model. Shaded areas depict 95% confidence intervals.

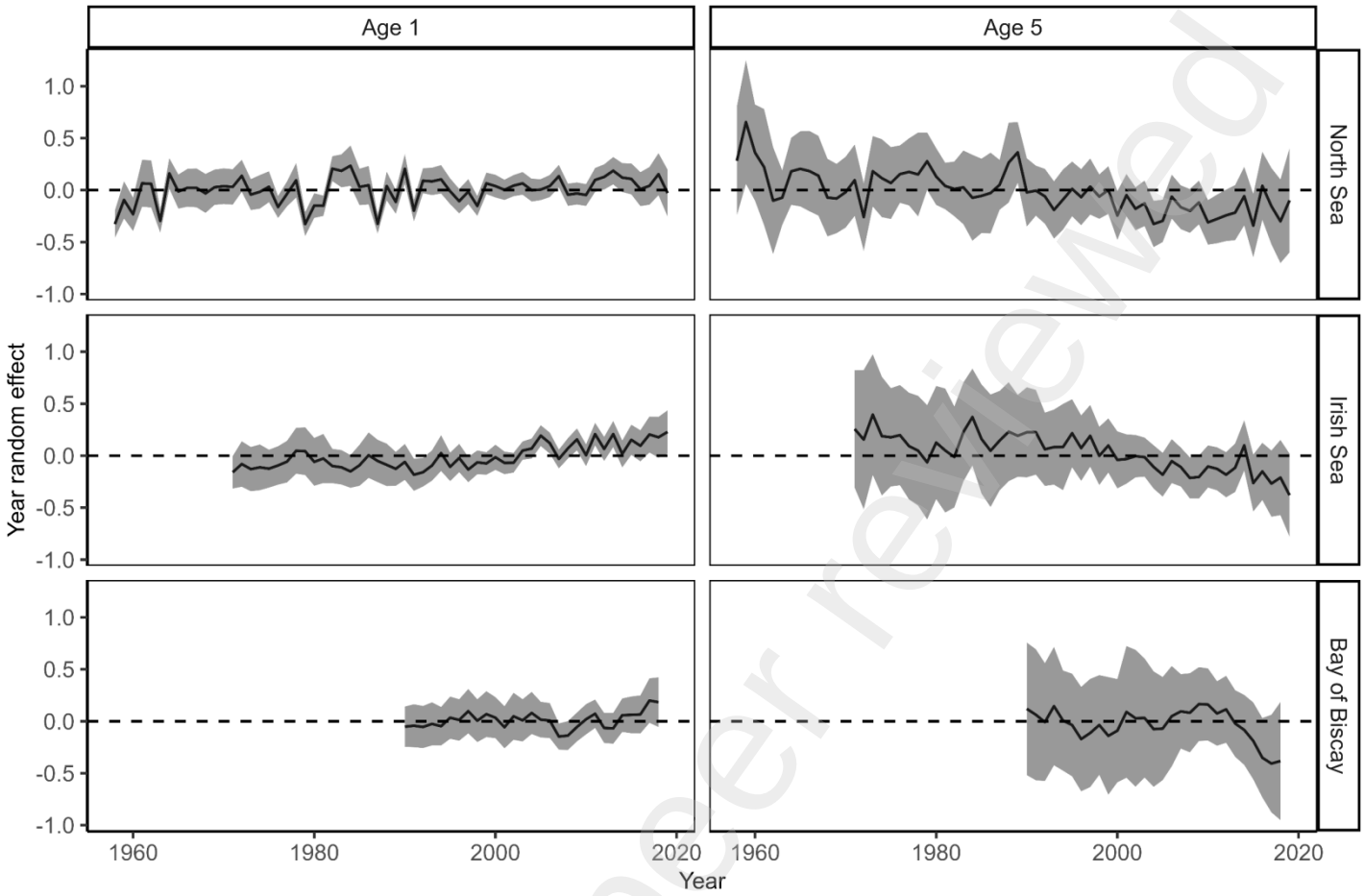

300

301 Figure 5. Temporal trends of sole growth represented by the year random effect from the best intrinsic model. Horizontal
302 dotted line represents the long-term average (intercept), with points above this line indicate good growth years while
303 points below this line indicate poor growth years. Shaded areas depict 95% confidence intervals.

	Intrinsic model	**Individual-level extrinsic model (ISIMIP)**	**Individual-level extrinsic model (ORAS5)**	**Individual-level extrinsic model (NEMO-MEDUSA)**
Fixed Effects	**Estimate (SE)**	**Estimate (SE)**	**Estimate (SE)**	**Estimate (SE)**
Intercept	7.85 (0.03)	7.74 (0.07)	7.80 (0.06)	7.77 (0.05)
ln(Age)	-1.22 (0.02)	-1.20 (0.02)	-1.22 (0.02)	-1.23 (0.02)

ln(Age at capture)	-0.15 (0.01)	-0.17 (0.01)	-0.16 (0.01)	-0.15 (0.01)
Reading Institute (WUR)	0.08 (0.03)	0.08 (0.03)	0.04 (0.03)	0.14 (0.04)
Reading Institute (WUR) * ln(Age)	-0.11 (0.02)	-0.11 (0.02)	-0.10 (0.02)	-0.14 (0.03)
Spawning Stock Biomass		0.46 (0.14)	0.30 (0.11)	0.32 (0.14)
Recruitment		0.11 (0.02)	0.08 (0.02)	0.05 (0.03)
Fishing mortality			-0.07 (0.06)	
$T_{individual\text{-}anomaly}$		-0.06 (0.04)	0.38 (0.07)	0.08 (0.04)
$T_{individual\text{-}anomaly}$ * ln(Age)		-0.13 (0.04)	-0.08 (0.03)	-0.20 (0.04)
$T_{individual\text{-}anomaly}$ * Spawning Stock Biomass		0.63 (0.15)		
$T_{individual\text{-}anomaly}$ * Recruitment				0.09 (0.03)
$T_{individual\text{-}anomaly}$ * Fishing mortality			-0.50 (0.13)	

$T_{individual\text{-}average}$		-0.04 (0.04)	-0.06 (0.02)	-0.13 (0.04)
$T_{individual\text{-}average}$ * ln(Age)		0.16 (0.04)		0.19 (0.04)
Random Effects				
σ^2	0.17	0.16	0.16	0.16
τ_{00}	0.01 $_{FishID}$	0.01 $_{FishID}$	0.01 $_{FishID}$	0.02 $_{FishID}$
	0.02 $_{Population:Year}$	0.02 $_{Population:Year}$	0.02 $_{Population:Year}$	0.03 $_{Population:Year}$
	0.00 $_{Population}$	0.01 $_{Population}$	0.01 $_{Population}$	0.00 $_{Population}$
τ_{11}		0.01 $_{Tindividual\text{-}anomaly\|FishID}$	0.03 $_{Tindividual\text{-}anomaly\|FishID}$	0.01 $_{Tindividual\text{-}anomaly\|FishID}$
	0.03 $_{ln(Age)\|Population:Year}$	0.04 $_{ln(Age)\|Population:Year}$	0.04 $_{ln(Age)\|Population:Year}$	0.04 $_{ln(Age)\|Population:Year}$
ρ_{01}		0.84 $_{FishID\text{-}ln(Age)}$	0.13 $_{FishID\text{-}ln(Age)}$	0.68 $_{FishID\text{-}ln(Age)}$
	-0.82 $_{Population:Year\text{-}ln(Age)}$	-0.85 $_{Population:Year\text{-}ln(Age)}$	-0.91 $_{Population:Year\text{-}ln(Age)}$	-0.92 $_{Population:Year\text{-}ln(Age)}$
N	2154 $_{FishID}$	2154 $_{FishID}$	2154 $_{FishID}$	1942 $_{FishID}$
	3 $_{Population}$	3 $_{Population}$	3 $_{Population}$	3 $_{Population}$
	62 $_{Year}$	62 $_{Year}$	62 $_{Year}$	40 $_{Year}$
Observations	15260	15260	15260	13367
Marginal R^2 / Conditional R^2	0.80 / 0.85	0.80 / 0.86	0.81 / 0.86	0.81 / 0.87

Table 3. Parameter estimates of the best intrinsic and individual-level extrinsic models. Estimates are given for fixed effects with standard error (SE). Residual variance (σ^2), the variance associated with tested effects (τ) and their correlations (ρ) are given for random effects.

3.2 Temperature effect: Population-level response vs. plasticity

There was no population-level response to spatial temperature variation ($T_{population\text{-}average}$ was not included in the final models). However, there was a population-level response to temporal temperature variation, which was derived from between-individual effect and plasticity (Figure 3F-N, **Error! Reference source not found.**). Despite the variation in magnitude across tested temperature datasets, population-level response to temporal temperature variation and plasticity were consistent with increasing juvenile growth (represented by age 1) and decreasing adult growth (from age 2-3 onwards, with an exception in the individual-level extrinsic model using ORAS5 data which is from age 7 onwards) at higher temperature. Best individual-level extrinsic models predicted that an increase of temperature by 1 degree was expected to increase age-1 growth by 3.2-16.2%, while decrease age-5 growth by 16.9-19.6% (models using ISIMIP and NEMO-MEDUSA data) or increase age-5 growth by 2.1% (model using ORAS5 data) (**Error! Reference source not found.**E-F). Between-individual effect was contrasting to plasticity. For the models using ISIMIP and NEMO-MEDUSA data, warmer period was associated with slower juvenile growth but faster adult growth (from age 2 onwards); for the model using ORAS5 data, warmer periods were associated with slower growth in both stages (**Error! Reference source not found.**C-D). In most ages, temperature was the extrinsic driver with the second strongest contribution to growth variation besides nutrients (Figure S18, Figure S19).

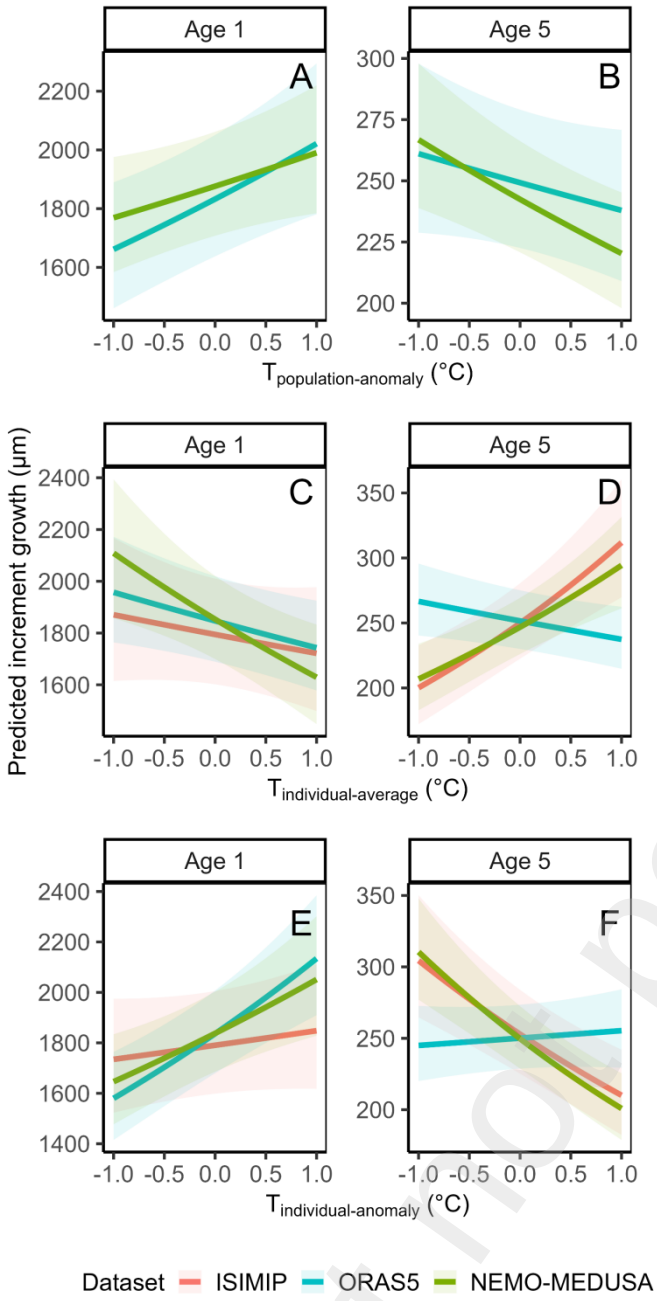

322

323 Figure 6. Predicted population-level growth response to temporal variation of temperature (A-B) from the best
324 population-level extrinsic models. Predicted growth plasticity to temperature (C-D) and between-individual effect (E-F)
325 from the best individual-level extrinsic models. Colours represent predicted effects from models using different
326 temperature datasets. Shaded areas depict 95% confidence intervals.

3.3 Environmental dependency of growth plasticity

Besides temperature effects, potential environmental drivers of fish growth (density, fishing pressure, nutrients) were tested in this study. A density effect was represented by spawning stock biomass and recruitment, and both showed positive effects without age interaction. An increase across the observed range of spawning stock biomass (0.02-0.46 [thousands/km^2]) and recruitment (0.01-2.53 [thousands/km^2]) was estimated to increase growth, respectively, by 14.2-22.5% and 13.3-31.2% (**Error! Reference source not found.**A-B). The positive effects of spawning stock biomass and recruitment remained even after accounting for nutrient data in the models (Table S11, Table S12). In addition, the effects were consistent when tested without standardising spawning stock biomass and recruitment (Figure S20). The effect of fishing pressure was not detected in population-level extrinsic models but showed a negative effect (5.7% across the observed range [0.02-0.87]) in the individual-level extrinsic model using ORAS5 data (**Error! Reference source not found.**C). Nutrients, represented by total phosphorus, showed positive effect with the strongest effect across examined extrinsic factors (Figure S19). An increase of total phosphorus from across the observed range (11.4-80.6 [kilotonne/year]) was estimated to increase growth by 31.2-38.8% (**Error! Reference source not found.**D).

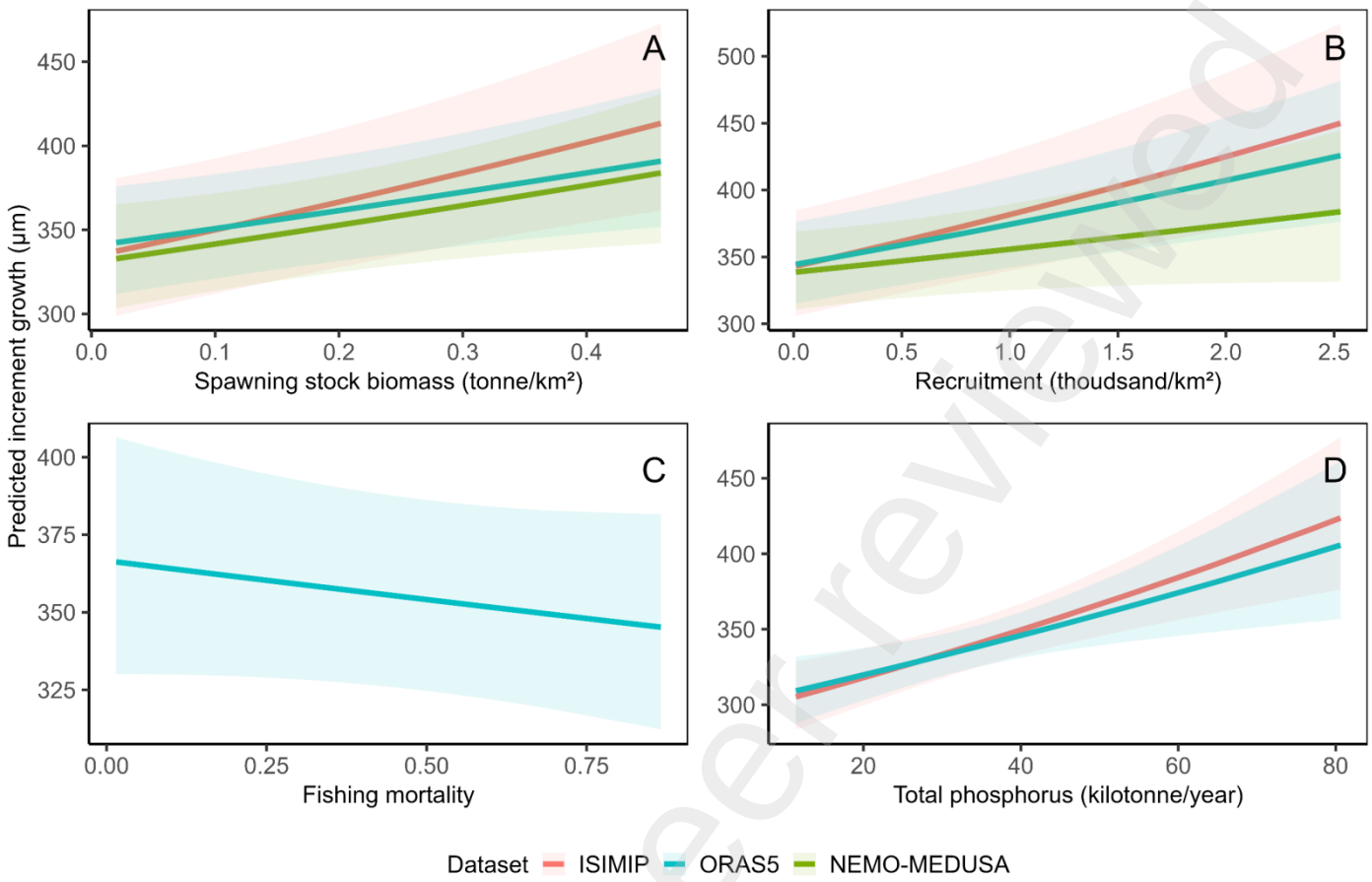

340

341 Figure 7. Predicted effects of spawning stock biomass (A), recruitment (B), fishing mortality (C), and total phosphorus (D)
342 from the best individual-level extrinsic models. Colours represent predicted effects from models using different
343 temperature datasets. Shaded areas depict 95% confidence intervals.

344 Regarding the environmental dependency of plasticity magnitude, the results showed no difference in plasticity
345 magnitude across population (random slope of $T_{individual\text{-}anomaly}$ for population was not included in the final models) but
346 across environmental conditions. Although the $T_{individual\text{-}anomaly}$-environment interaction terms differed across tested
347 temperature datasets, there was a common pattern that in environmental conditions that are favourable for growth
348 (higher spawning stock biomass and recruitment, lower fishing mortality) plasticity was stronger for younger ages but
349 milder for older ages (**Error! Reference source not found.**).

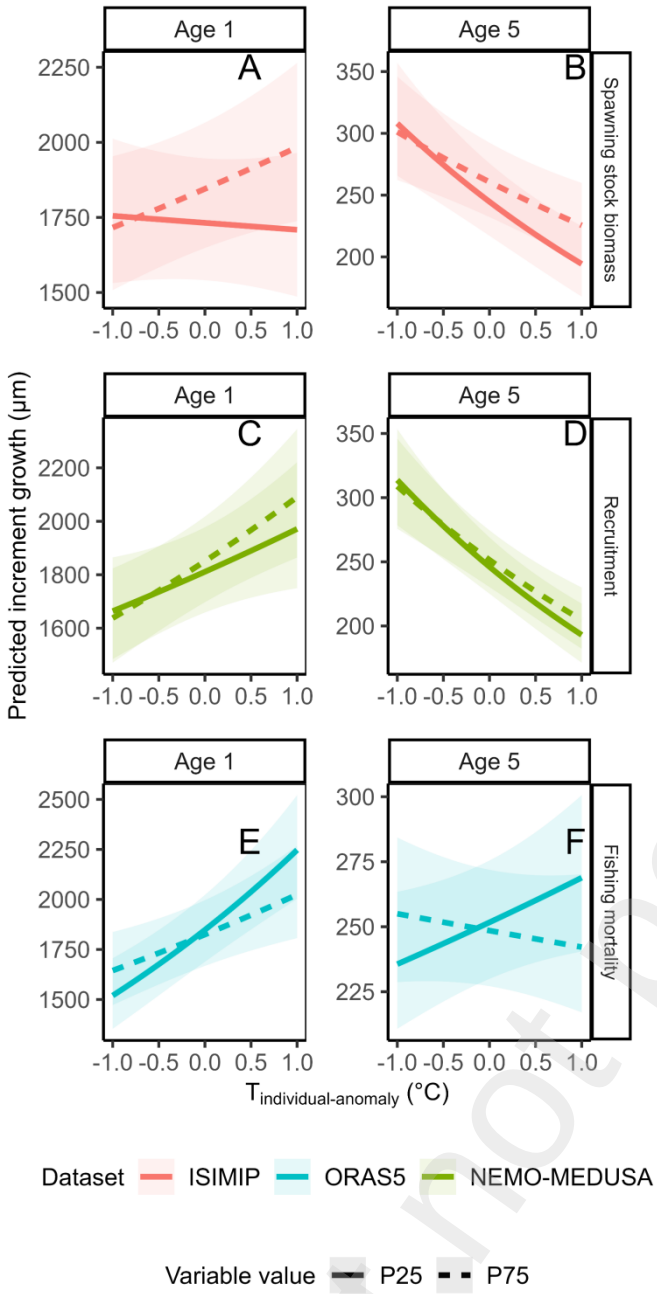

350

351 Figure 8. Predicted growth plasticity to temperature under different levels of spawning stock biomass (A-B), recruitment
352 (C-D), and fishing mortality (E-F) from the best individual-level extrinsic models. Colours represent predicted effects from
353 models using different temperature datasets. P25 and P75 refer to the 25% and 75% percentile value of observed
354 spawning stock biomass, recruitment, and fishing mortality. Shaded areas depict 95% confidence intervals.

355 Regarding the environmental dependency of individual plasticity variance, the results showed difference in individual
356 plasticity variance across population and environmental conditions. The variance of individual growth plasticity in North

Sea and Irish Sea populations was estimated to be 1.43-3.27 times and 1.27-1.68 times higher than in Bay of Biscay population, respectively (estimated from data subsets with increment measurement range 2-11 and 6-11) (**Error! Reference source not found.**). Notably, the estimates were higher in the model using ORAS5 data, especially in the comparison between North Sea and Bay of Biscay populations. There was no consistency across tested temperature datasets in the variance difference between North Sea and Irish Sea populations. The model using ISIMIP, ORAS5, and NEMO-MEDUSA data showed no difference, higher variance, and lower variance in the North Sea compared to in the Irish Sea, respectively (**Error! Reference source not found.**). Although the correlation tests showed variable results, there was a consistent negative correlation between cohort-specific variance of individual plasticity and spawning stock biomass and recruitment in the Irish Sea (Figure S21).

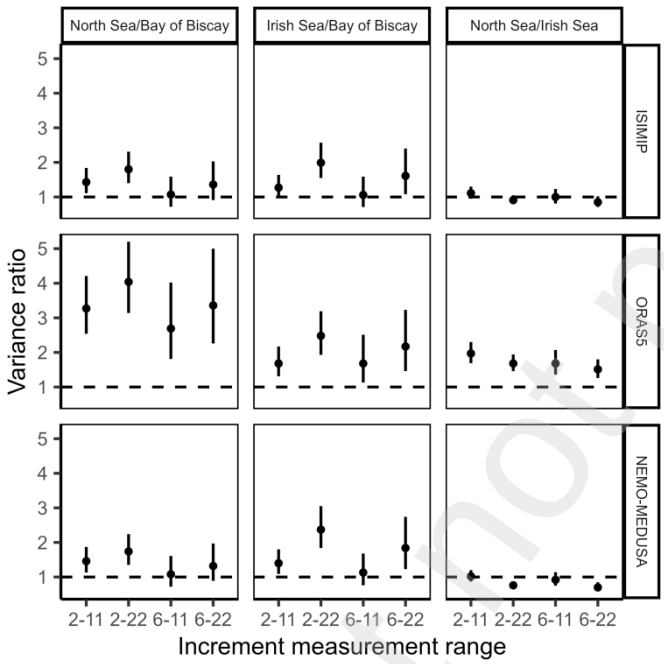

Figure 9. Predicted variance ratio of individual growth plasticity to temperature for each population pairs (North Sea/Bay of Biscay, Irish Sea/Bay of Biscay, North Sea/Irish Sea) from models using different temperature datasets.

4 Discussion

4.1 Fish growth plasticity to temperature

Our results on *Solea solea* provide support for growth plasticity to temperature following the TSR, i.e. fish grow faster at juvenile but slower at adult stage at warmer temperature (Atkinson, 1994). The mechanism of the TSR remains debatable

with two major hypotheses. The first hypothesis is based on the limitation perspective where growth is modelled as a difference between anabolism and catabolism and it is assumed that the response rate to increasing temperature of catabolism is higher than that of anabolism (Pauly, 2021; Pauly and Cheung, 2018; Perrin, 1995; von Bertalanffy, 1938). The second hypothesis is based on optimisation (or life-history) perspective that at higher temperature ectotherm organisms will optimise their growth-reproduction trade-offs as a response to the expectation of higher mortality, which is referred to as ghosts of evolutionary past (Angilletta et al., 2004; Kozłowski et al., 2004; Verberk et al., 2021). Both hypotheses have support and criticism, and it has been proposed that mechanistic explanation of the TSR should reconcile both perspectives (Audzijonyte et al., 2022).

We argue that the increase of juvenile growth can be linked to the increase of energy intake, while the decrease of adult growth can be linked to the trade-off between growth and reproduction. Feeding and consumption rate in juvenile sole was found to increase with temperature and decrease when temperature exceeds the optimal growth temperature (Schram et al., 2013; Vinagre et al., 2007). The maximum increase of temperature in our study is about 1.3^{o}C above the long-term annual average of 9.1-12.8^{o}C. The temperature in our study, which is aggregated over the whole distribution of sole, may underestimate the actual temperature experienced by juvenile sole in coastal or nursery area. However, we do not expect an increase of temperature above the optimal growth temperature of juvenile sole, which is in the range of 20-25^{o}C (Fonds, 1976; Schram et al., 2013). Experiments and simulation studies indicate that the baseline metabolic rate of sole increases exponentially with increasing temperature (Fonseca et al., 2010; Lefrancois and Claireaux, 2003). In our study, it is unlikely that the decrease of adult growth is due to metabolic constraint at high temperature as the temperature range in our study is expected to be within the optimal metabolic temperature of adult sole of about 19^{o}C (Lefrancois and Claireaux, 2003). However, we cannot completely rule out the possibility of metabolic limitation because the actual optimal growth temperature may be much lower than the optimal metabolic temperature (Clark et al., 2013). A more plausible explanation for the decrease of adult growth at higher temperature can be the increase of reproductive investment as we found that sole growth starts to decrease with temperature from age 2-3 onwards, which is the onset of sole maturation reported in literature (Mollet et al., 2013; Mollet et al., 2007).

Our results showed that population-level response to temporal temperature variation was derived from both plasticity and between-individual effect, which is consistent with other studies on fish growth (Morrongiello et al., 2019; Smoliński

et al., 2020a). Especially, in the analysis using ISIMIP data, a population-level response was not detected, because plasticity and between-individual cancelled each other out. This emphasizes that in field studies it is not always possible to infer plasticity from population-level analyses (Nussey et al., 2007; van de Pol and Wright, 2009). Thus, long-term collection of individual-based data and hierarchical models (e.g. mixed-effects model) are crucial to scrutinize analyses of individual plasticity.

In addition to quantifying growth plasticity to temperature, mixed-effect models allowed us to quantify different levels of temperature effect, i.e. spatial temperature variation across populations and between-individual effect. Our results provide support that the systematic difference in growth across populations is not due to temperature difference, which contrasts with the results from Mollet et al. (2013). This may be explained by the smaller magnitude of difference detected in our study versus the wide variability in energy acquisition (0.9-22.3%) reported by Mollet et al. (2013). The between-individual effect individuals contrasted with plasticity, i.e. slower juvenile growth but faster adult growth at warmer temperature. While the negative effect in juvenile is difficult to interpret, the positive effect in adult may be due to a more favourable environment for sole growth associated with the increases of average temperature, e.g. increasing in abundance of major preys such as polychaetes and crustaceans (Kröncke et al., 2011).

4.2 Environmental dependency of growth plasticity to temperature

We included a series of potential factors affecting growth (density, fishing pressure, nutrients) to control for their confounding effects on the TSR and test for the environmental dependency of growth plasticity to temperature. We found positive effects of spawning stock biomass and recruitment on growth, which persisted even after accounting for the effect of nutrients. These results are surprising as we expect growth to be slower at higher density due to intraclass competition. A negative density-growth relationship in sole has been observed in juveniles (in experimental setting) (Lund et al., 2013) and in adults (Rijnsdorp and Van Beek, 1991), while a few studies found no effect of density on growth (Millner and Whiting, 1996; Rogers, 1994; Teal et al., 2008). Thus, the positive effects of spawning stock biomass and recruitment on growth unlikely represent density effect but may be linked to trends of one or more confounding factors, such as food availability, which may not only be affected by nutrients but also by seabed disturbance of fishing (Hiddink et al., 2006; Hiddink et al., 2016; Rijnsdorp and Vingerhoed, 2001). Regarding the effect of fishing pressure, we only found a weak negative effect in the individual-level extrinsic model using ORAS5 data but a negative effect of age at capture in all

models. It is likely that the effect of age at capture, in most cases, recorded the effect of fishing and represented the selectivity of fishing for fast-growing fish that can attain the catchable size earlier. There has been empirical support for fisheries-induced evolution of earlier maturation in sole in the North Sea (Mollet et al., 2007) and of slower growth in other exploited species such Atlantic cod (Neuheimer and Grønkjær, 2012; Swain et al., 2007), haddock (Neuheimer and Taggart, 2010; Wright et al., 2011), European plaice (Van Walraven et al., 2010), and anchovy (Boëns et al., 2023).

Growth plasticity to temperature varied, both in terms of magnitude and variance, across environmental conditions. Under favourable conditions for sole growth (lower fishing pressure, higher spawning stock biomass and recruitment), individual plasticity to temperature showed stronger positive response, weaker negative response, and lower variance. These are consistent with the results of previous studies (Morrongiello et al., 2021; Smoliński et al., 2020b). The variation of individual plasticity can be derived from both genetic and ecological causes (Nussey et al., 2007). In our study, the different magnitude of plasticity at different fishing levels may be linked to genetic cause. At lower fishing pressure, there can be more fast-growing individuals, who may express stronger response to temperature in the populations and thus lead to an improvement in the average response. Meanwhile, the difference in both magnitude and variance of plasticity at different spawning stock biomass and recruitment may be linked to ecological cause. Higher spawning stock biomass and recruitment, which were associated with faster growth, may represent favourable conditions for growth rather than density constraint (see discussion above) and consequently facilitates stronger and lower variance of individual plasticity. Campana et al. (2022) has indicated that the growth strategy of fish can be environmentally dependent, whereby growth variance decreases during favourable conditions to maximise growth but increases during unfavourable conditions to increase buffering capacity of the population.

Another interesting result is that there was no difference in magnitude but in variance of plasticity across populations. The results provide strong support for higher variance of individual plasticity in the North Sea and the Irish Sea than in the Bay of Biscay. Morrongiello et al. (2019) found a difference in the variance of individual plasticity within populations before and after the onset of fishing. However, this is unlikely the case in our study given the relatively similar magnitude and trend of fishing mortality in the populations under study. A plausible reason may be the difference in environmental heterogeneity (De Jong, 2005; Ghalambor et al., 2007), which was suggested in studies in phenotypic plasticity of great tit *(Parus major)* (Portlier 2012, Husby 2010). In our study, the variance of $T_{population\text{-}anomaly}$ was significantly lower in the Bay

of Biscay compared to other areas (except for when compared to the Irish Sea in the analysis using ORAS5 data) (Table S13).

Understanding the environmental dependency of individual plasticity is crucial to predict future response of life-history trait (e.g. growth) to environmental change (e.g. warming) (Nussey et al., 2007). Our results indicate that if the environmental conditions remain unfavourable for sole growth, represented by low spawning stock biomass and recruitment, the positive response of juvenile growth is expected to be diminished while the negative response of adult growth is expected to be amplified; and these trends may be mitigated by keeping fishing at low level. In addition, population-specific resilience to future climate change may be different due to the difference in individual plasticity variance.

5 Conclusions

The response of sole growth to temperature was found to be a complex process involving both plasticity and between-individual effects. Growth plasticity followed the TSR and was dependent on environmental conditions, both in terms of plasticity magnitude and individual plasticity variance. Our study provides not only additional support for the universality of the TSR but also contributed to our understanding of growth plasticity to temperature and responses of fish populations to current and future climate change.

6 Acknowledgements

This work was supported by the Research Foundation - Flanders (FWO) in the form of PhD Fellowship fundamental research awarded to the first author. We gratefully thank all the staff involved in the collection, process, and archive of otolith data at ILVO, WUR, and IFREMER; Ilse Maertens for her expertise in otolith reading; Klaas Sys and Charlotte Van Moorleghem for their help with the temperature, survey, and nutrient data. The study also benefitted from the scientific network of the H2020 project SEAwise (Societal challenges, GA number 101000318).

7 Data availability

Data will be made available on request. R code to reproduce the results reported in this paper are available on Github (https://github.com/Anhbt95/FWO-PhD_WP1_Growth-linear-mixed-model).

8 Appendix A. Supplementary data

Appendix S1. Growing cycle of sole otolith

The formation of sole otolith starts when fish is hatched (Amara et al., 1994) (a few days after spawning (Pawson, 1995)). Since average spawning period ranges from early February in the Bay of Biscay (Amara et al., 1994; Vaz et al., 2019; Vinagre et al., 2008) to late May in the North Sea (Fincham et al., 2013; Lacroix et al., 2013; Rijnsdorp and Vingerhoed, 1994), the hatch time and otolith formation time vary approximately between February and May depending on the region. One growing cycle starts when the formation of the opaque ring (often referred to as summer ring) begins and ends when the formation of the translucent ring (winter ring) finishes (Black et al., 2005; Millner et al., 2011; Millner and Whiting, 1996). For sole, the opaque zone of sole otolith usually forms in May-October while the translucent zone usually forms in November-April (Millner and Whiting, 1996). One complete growing cycle or otolith ring is counted from the *nucleus* to the end of the first translucent ring, or from the end of one translucent ring to the end of the subsequent translucent ring.

Since the otolith formation is seasonal, the information of capture month and of the edge form (opaque or translucent) is used for age determination:

- January-April: translucent ring is usually completing. The last ring is not a complete ring yet but is still counted as 1 age (**Error! Reference source not found.**).
- May-June: translucent ring is usually completed and new opaque otolith ring is starting. The last ring is usually a complete ring and is counted as 1 age (**Error! Reference source not found.**).
- July-December: new opaque otolith ring is usually starting. The last ring is not counted as 1 age (**Error! Reference source not found.**)

Figure S1. Sole otolith (preparation method: broken/burned; estimated age: 6; month of capture: February; location: Irish Sea; ID: SOL_123_1999-02-19_Z.284_19-02-1999_2110). The last ring has translucent edge, is completing, and is counted as 1 age.

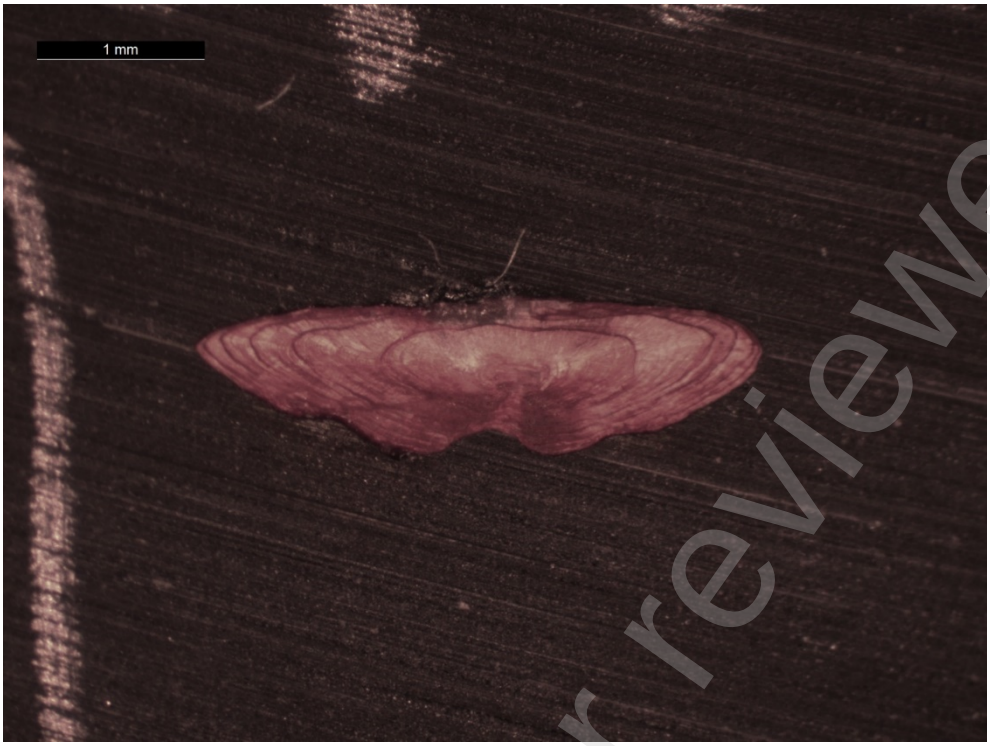

Figure S2. Sole otolith (preparation method: sectioned/stained; estimated age: 6; month of capture: February; location: Irish Sea; ID: 92BA82C4-D801-494D-A896-D2E9CC9F2399). The last ring has translucent edge, is completing, and is counted as 1 age.

Figure S3. Sole otolith (preparation method: sectioned/stained; estimated age: 6; month of capture: June; location: Irish Sea; ID: D31B65C5-8C67-409B-A841-4E39C41637E3). The last ring on the left has translucent edge and is completing. The last ring on the right is completed and new ring is starting. The last ring is counted as 1 age.

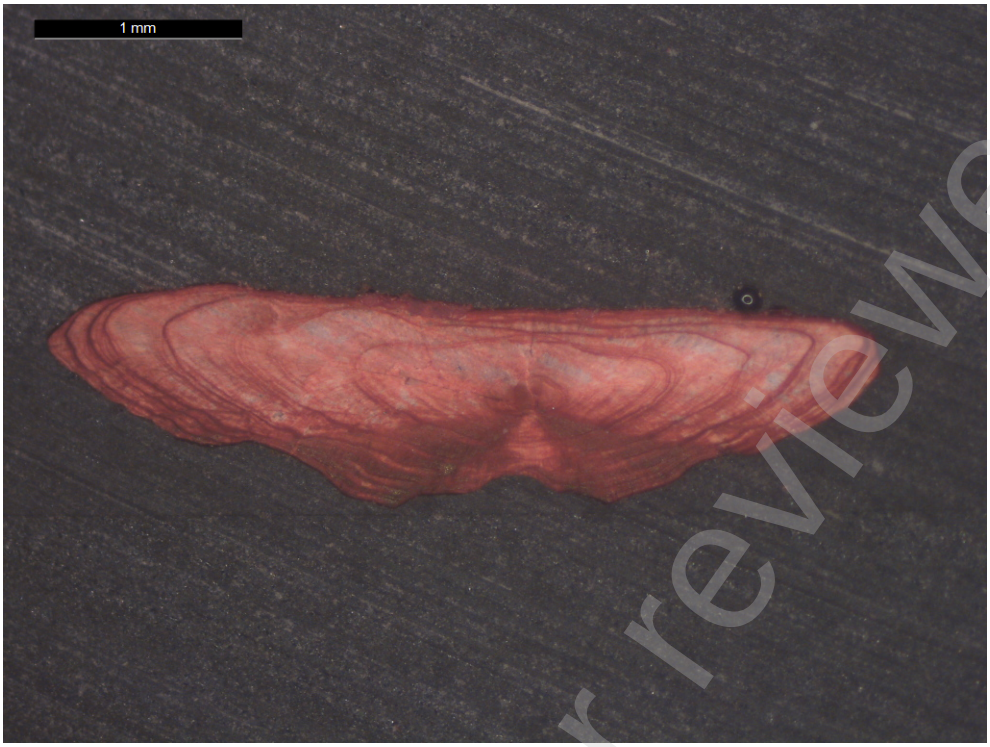

Figure S4. Sole otolith (preparation method: sectioned/stained; estimated age: 6; month of capture: October; location: North Sea; ID: B766C47E-1BA1-465C-9B5E-752F9D1C26D). The last ring has translucent edge, is not completed, and is not counted as 1 age.

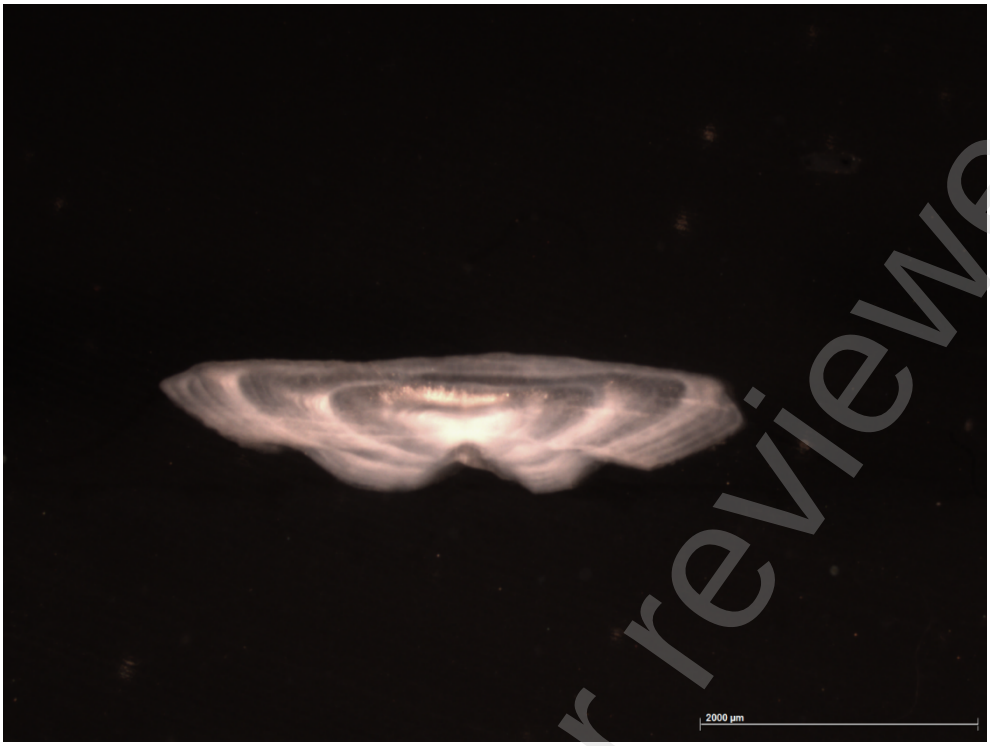

Figure S5. Sole otolith (preparation method: sectioned; estimated age: 6; month of capture: February; location: Bay of Biscay; ID: CO_16_B34_C1_O_0001). The last ring has translucent edge, is completing, and is counted as 1 age.

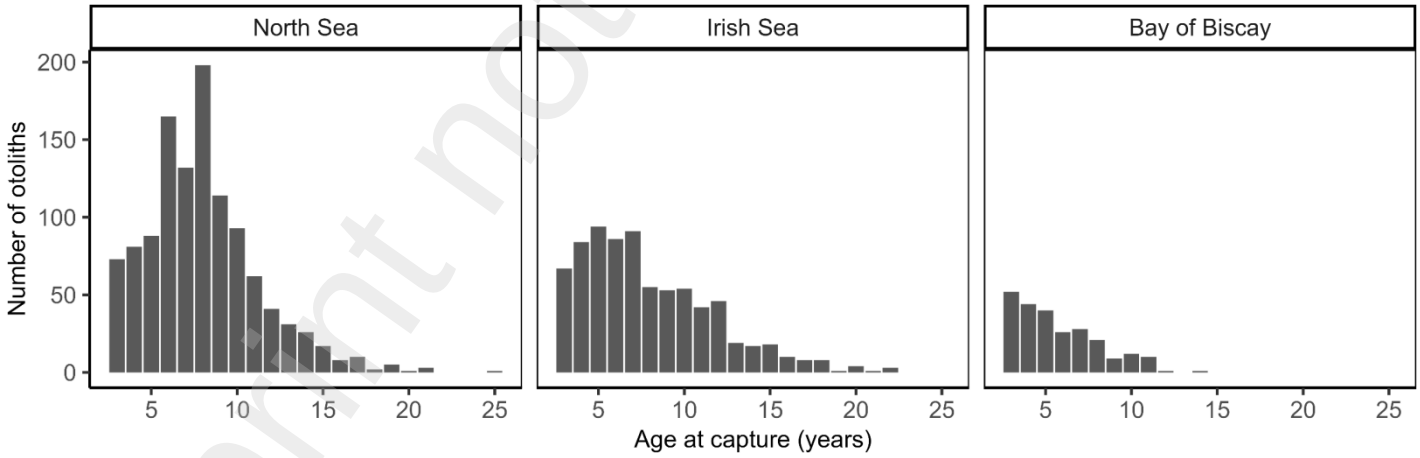

Figure S6. Distribution of age at capture by population.

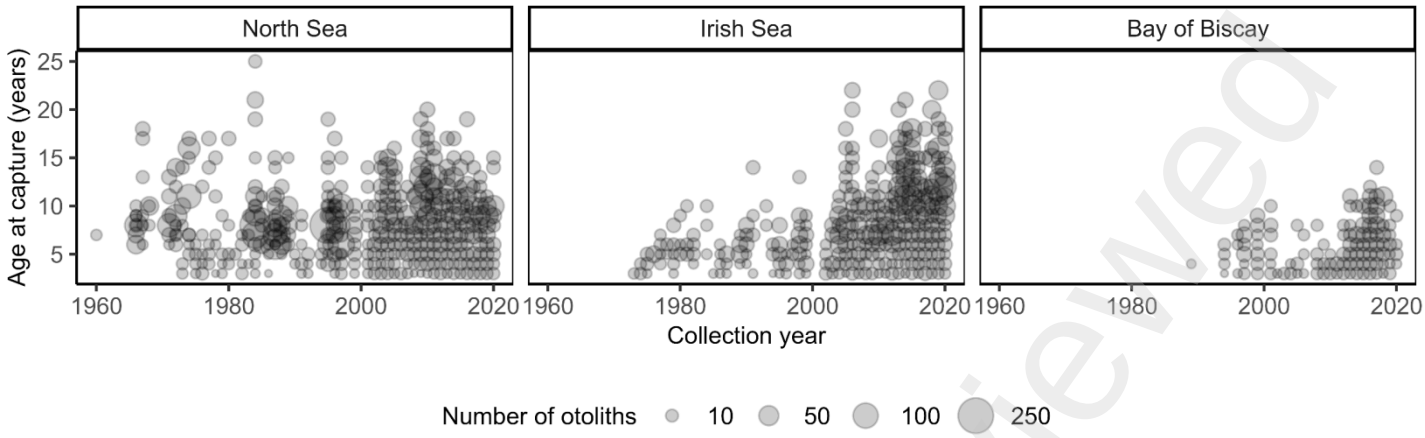

Figure S7. Number of sampled otoliths by population, collection year, and age at capture.

Table S1. Aging consistency between two readers Tuan Anh Bui and Kelly Díaz, and an experienced expert at ILVO. The aging is considered precise as the coefficient of variations are under 5% (Campana, 2001).

Reader	Number of aged otoliths	Number of re-age otoliths	Coefficient of variation
Tuan Anh Bui	1481	1477	0.67%
Kelly Díaz	244	240	2.02%

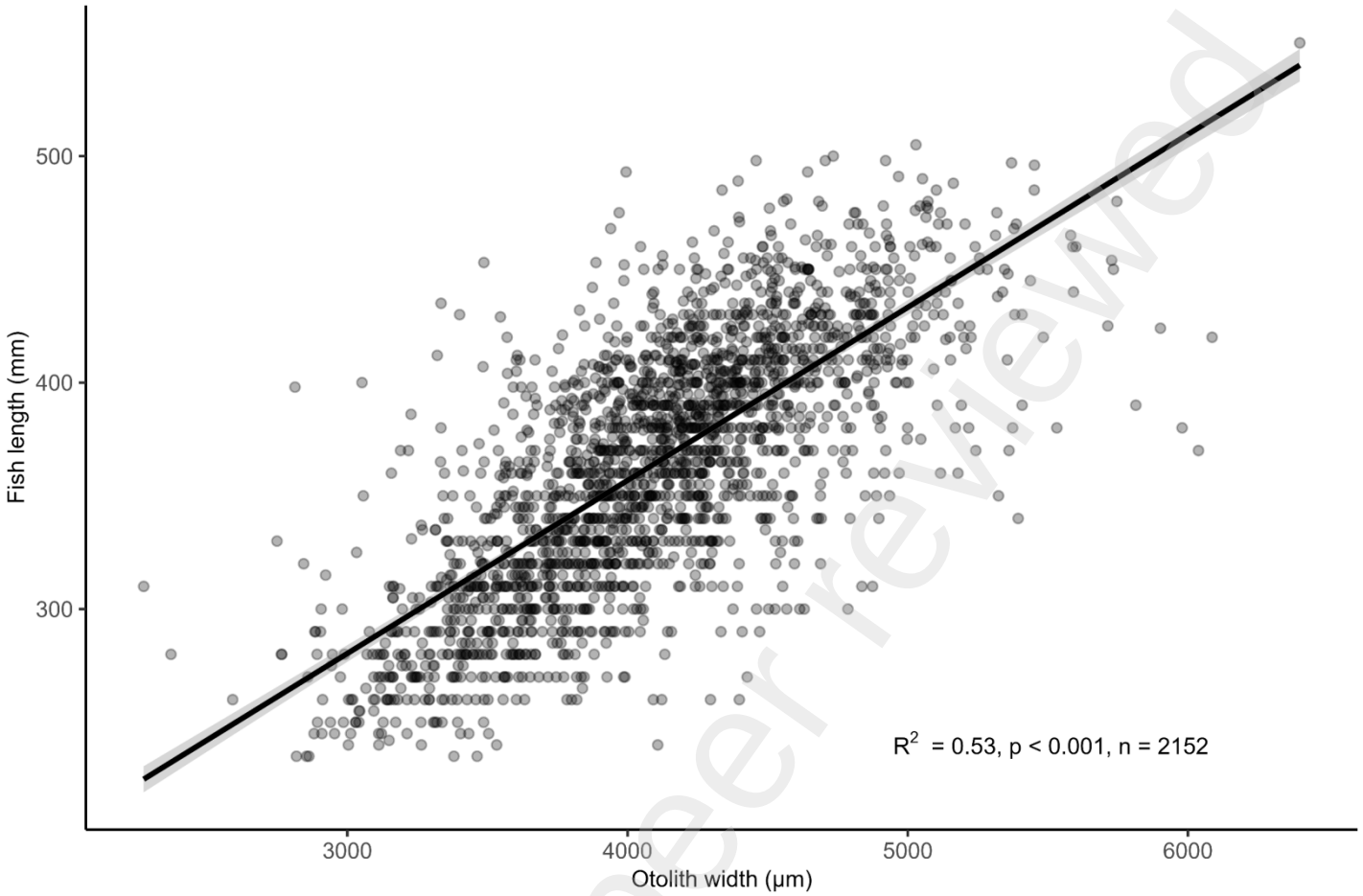

Figure S8. Correlation between otolith width and fish length. The correlation test excluded 2 otoliths with very small otolith width (< 1500 µm) which is likely due to error in the database.

Appendix S2. Correlation between modelled and *in situ* temperature.

In situ bottom temperature was extracted from the International Council for the Exploration of the Sea (ICES) High Resolution CTD data (1970-2021) (ICES, 2022). *In situ* data are scattered over space and time, and are generally more available in the recent years (**Error! Reference source not found.**). For each modelled temperature dataset (ISIMIP, ORAS5, NEMO-MEDUSA), we matched *in situ* data at a certain day and a certain latitude-longitude coordinate with modelled data at a certain month and a certain grid cell that contains the *in situ* location(s) (**Error! Reference source not found.**). For the data that match, we regressed modelled data on *in situ* data to assess their correlation.

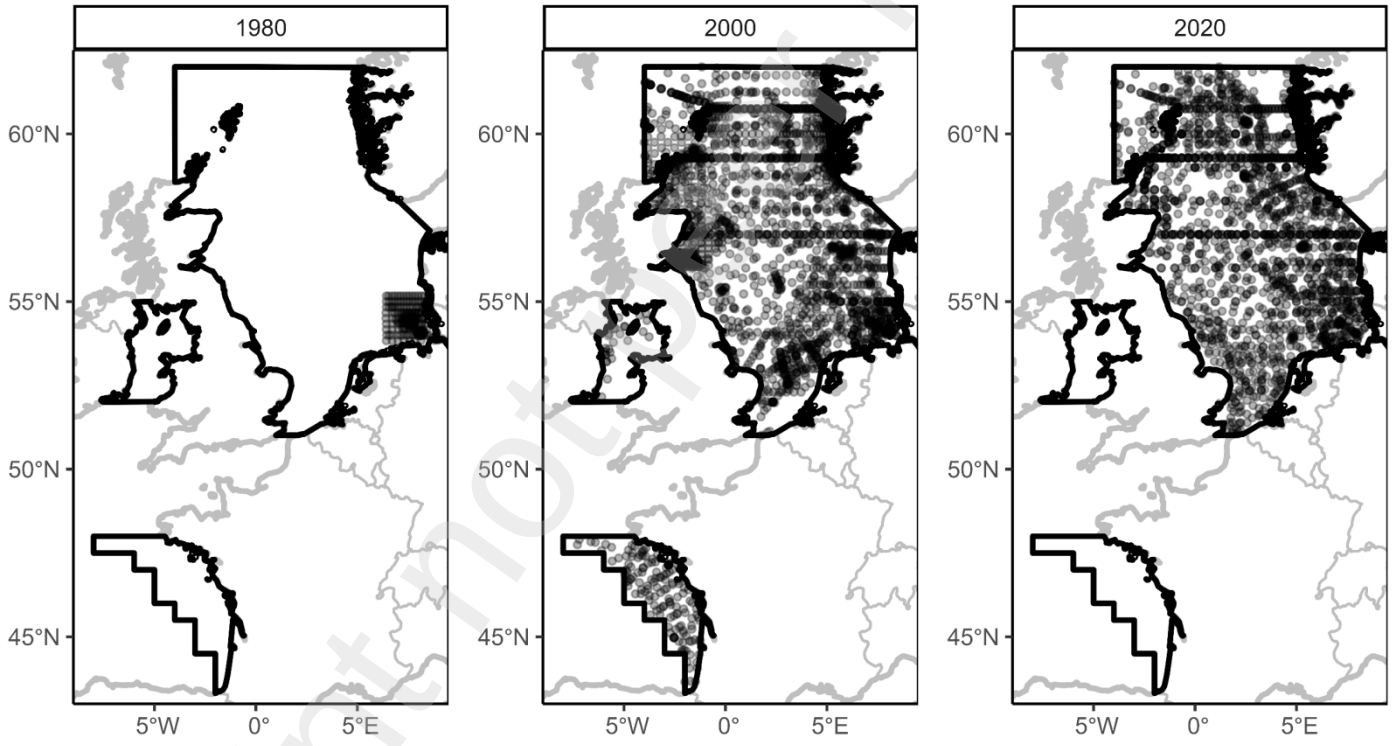

Figure S9. Locations of *in situ* bottom temperature data from the ICES High Resolution CTD data. Polygons with solid line indicates the stock management areas.

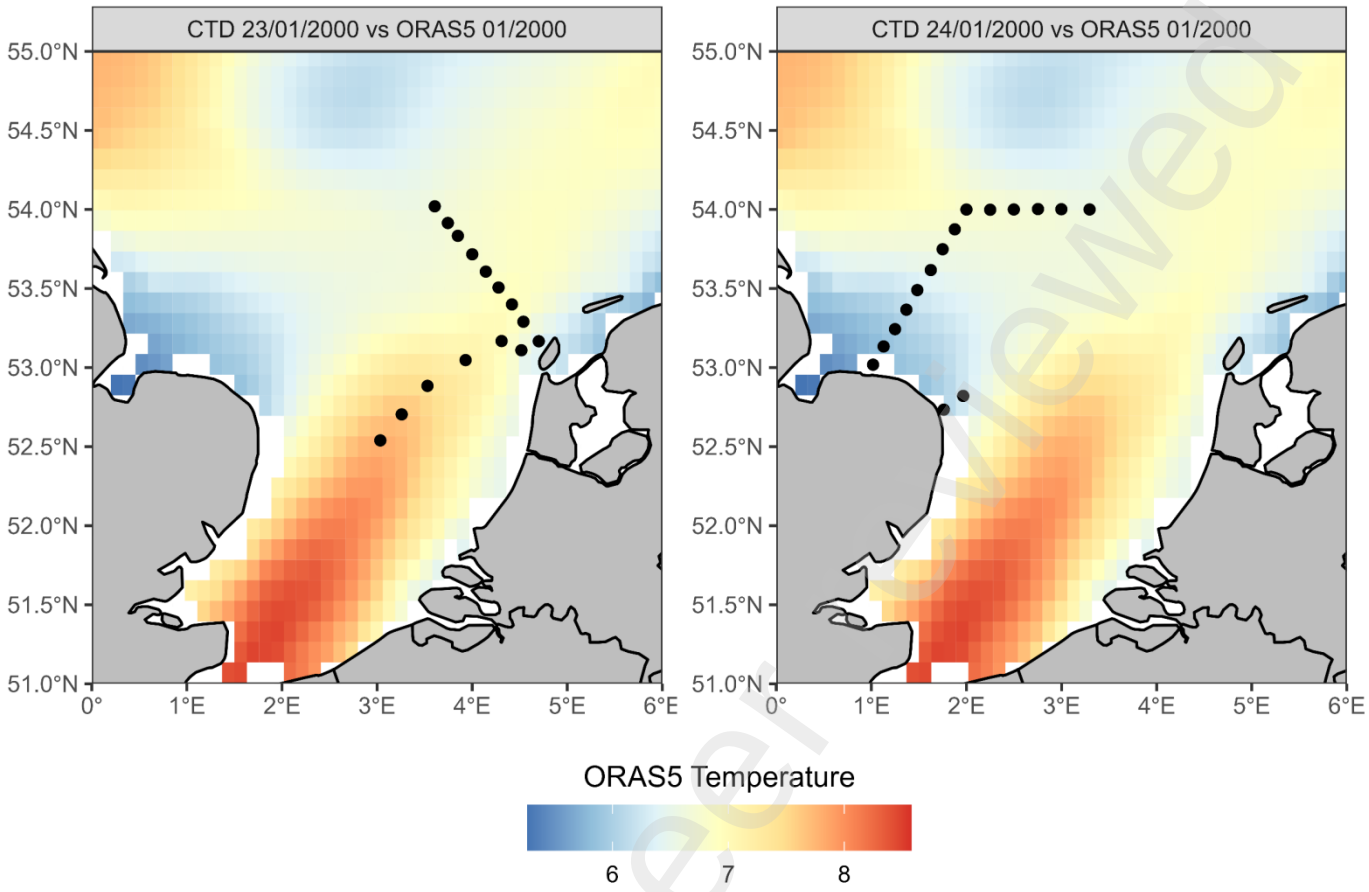

Figure S10. Examples of the matching between *in situ* data (point) and modelled data (grid cell). White cells indicates no modelled data available.

Table S2. R^2 from the regression of modelled data on *in situ* data.

Temperature dataset	**North Sea**	**Irish Sea**	**Bay of Biscay**
ISIMIP	0.87	0.76	0.31
ORAS5	0.96	0.93	0.54
NEMO-MEDUSA	0.88	0.77	0.50

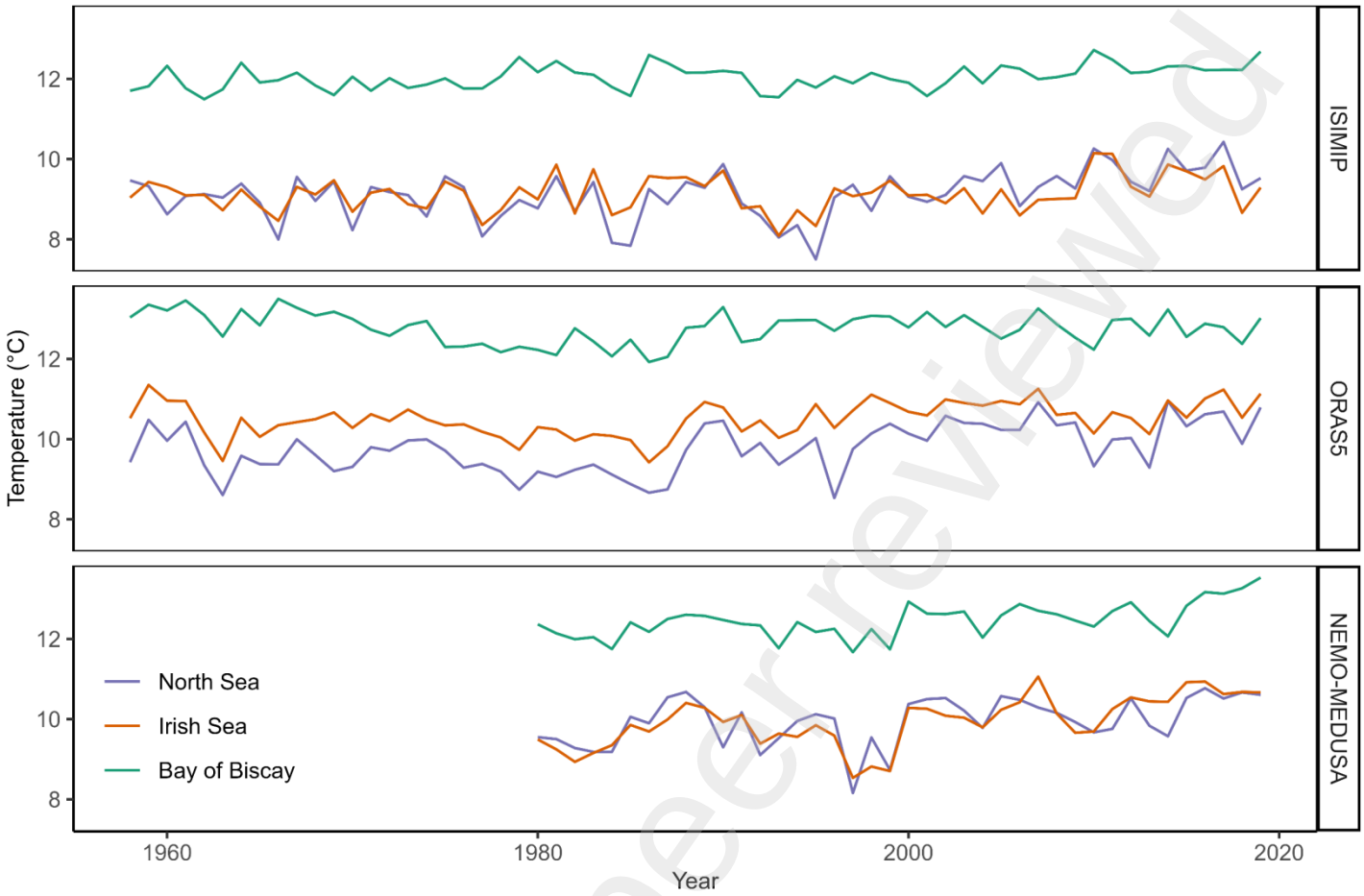

Figure S11. Temporal trend of mean annual temperature (within the distribution areas).

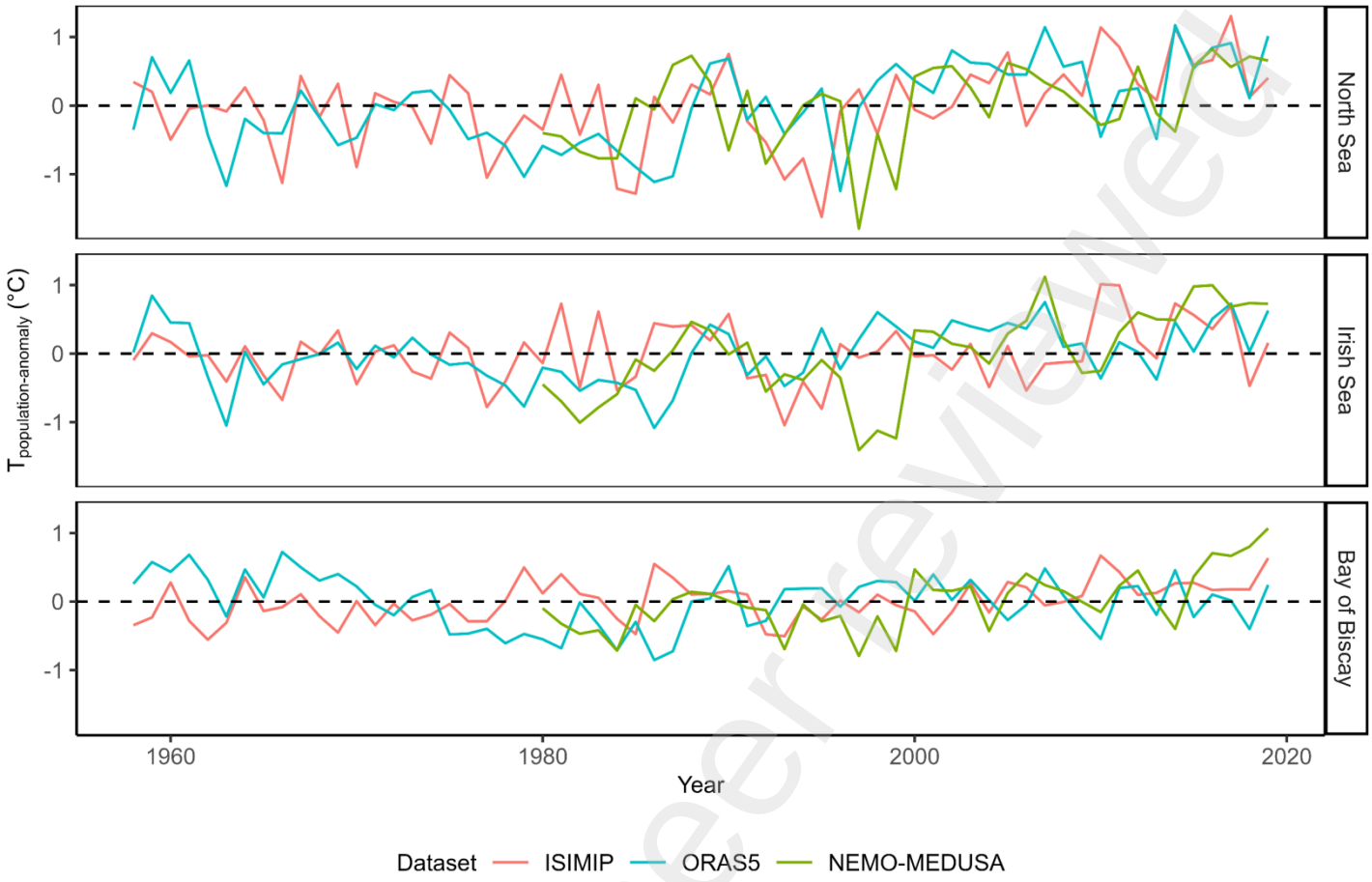

Figure S12. Temporal trend of population-specific temperature anomaly ($T_{population\text{-}anomaly}$).

Table S3. Correlation between annual mean temperatures and seasonal mean temperatures.

Season	Temperature dataset	Population	R^2	p-value

Summer (Jun-Aug)	ISIMIP	North Sea	0.80	0
Summer (Jun-Aug)	ISIMIP	Irish Sea	0.87	0
Summer (Jun-Aug)	ISIMIP	Bay of Biscay	0.93	0
Summer (Jun-Aug)	ORAS5	North Sea	0.86	0
Summer (Jun-Aug)	ORAS5	Irish Sea	0.80	0
Summer (Jun-Aug)	ORAS5	Bay of Biscay	0.89	0
Summer (Jun-Aug)	NEMO-MEDUSA	North Sea	0.91	0
Summer (Jun-Aug)	NEMO-MEDUSA	Irish Sea	0.96	0
Summer (Jun-Aug)	NEMO-MEDUSA	Bay of Biscay	0.93	0
Autumn (Sep-Nov)	ISIMIP	North Sea	0.51	0
Autumn (Sep-Nov)	ISIMIP	Irish Sea	0.76	0
Autumn (Sep-Nov)	ISIMIP	Bay of Biscay	0.79	0
Autumn (Sep-Nov)	ORAS5	North Sea	0.58	0
Autumn (Sep-Nov)	ORAS5	Irish Sea	0.74	0
Autumn (Sep-Nov)	ORAS5	Bay of Biscay	0.79	0

Autumn (Sep-Nov)	NEMO-MEDUSA	North Sea	0.54	0
Autumn (Sep-Nov)	NEMO-MEDUSA	Irish Sea	0.82	0
Autumn (Sep-Nov)	NEMO-MEDUSA	Bay of Biscay	0.81	0
Winter (Dec-Feb)	ISIMIP	North Sea	0.65	0
Winter (Dec-Feb)	ISIMIP	Irish Sea	0.74	0
Winter (Dec-Feb)	ISIMIP	Bay of Biscay	0.81	0
Winter (Dec-Feb)	ORAS5	North Sea	0.75	0
Winter (Dec-Feb)	ORAS5	Irish Sea	0.71	0
Winter (Dec-Feb)	ORAS5	Bay of Biscay	0.74	0
Winter (Dec-Feb)	NEMO-MEDUSA	North Sea	0.79	0
Winter (Dec-Feb)	NEMO-MEDUSA	Irish Sea	0.89	0
Winter (Dec-Feb)	NEMO-MEDUSA	Bay of Biscay	0.81	0
Spring (Mar-May)	ISIMIP	North Sea	0.84	0
Spring (Mar-May)	ISIMIP	Irish Sea	0.85	0
Spring (Mar-May)	ISIMIP	Bay of Biscay	0.89	0

Spring (Mar-May)	ORAS5	North Sea	0.85	0
Spring (Mar-May)	ORAS5	Irish Sea	0.81	0
Spring (Mar-May)	ORAS5	Bay of Biscay	0.87	0
Spring (Mar-May)	NEMO-MEDUSA	North Sea	0.89	0
Spring (Mar-May)	NEMO-MEDUSA	Irish Sea	0.93	0
Spring (Mar-May)	NEMO-MEDUSA	Bay of Biscay	0.93	0

Appendix S3. Sole distribution areas estimated from beam trawl survey data.

We collected data from four beam trawl surveys: Beam Trawl Survey (BTS), Beam Trawl Survey in the Bay of Biscay (BTS-VIII), Inshore Beam Trawl Survey (DYFS), and Sole Net Survey (SNS) (DATRAS, 2023). Data were downloaded for the period

1985-2022 (DATRAS, 2023). The distribution areas of sole were determined as all ICES statistical rectangle (0.5° x 1° latitude-longitude resolution) with presence of sole.

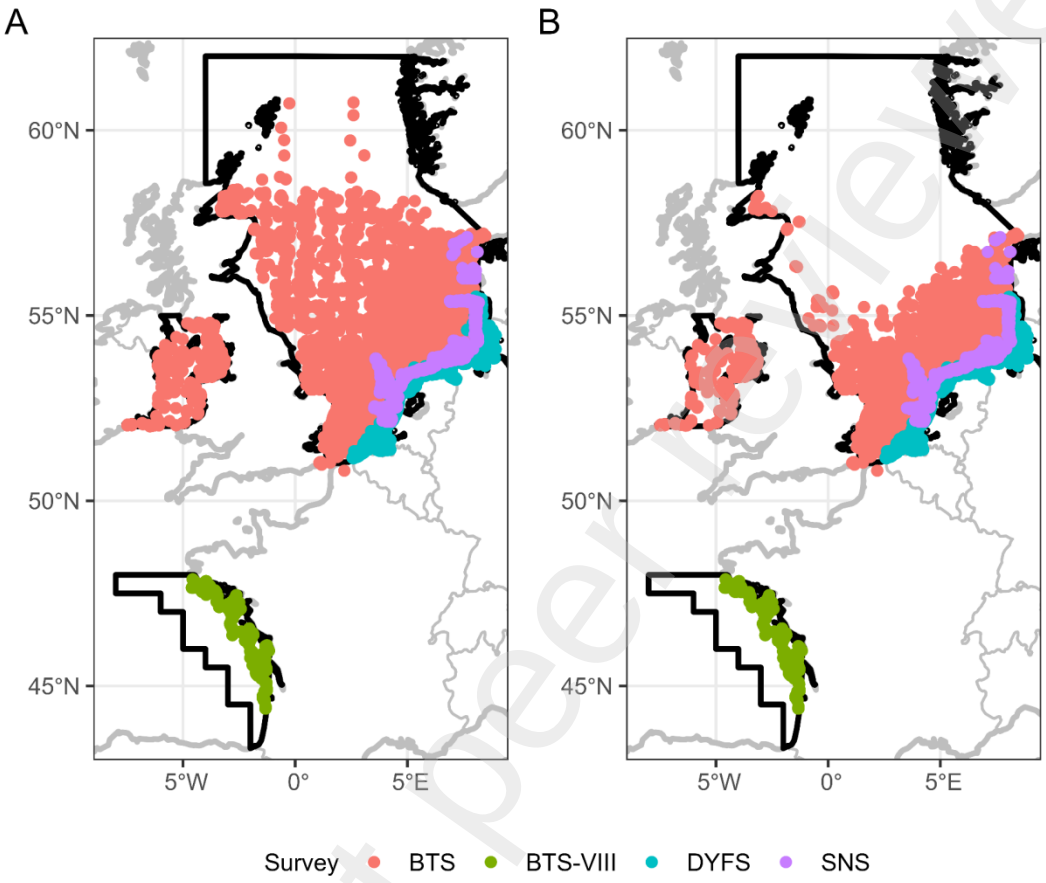

Figure S13. Sampling haul locations of beam trawl surveys (A) and locations with presence of sole (B). Colours represent different surveys: Beam Trawl Survey (BTS), Beam Trawl Survey in the Bay of Biscay (BTS-VIII), Inshore Beam Trawl Survey (DYFS).

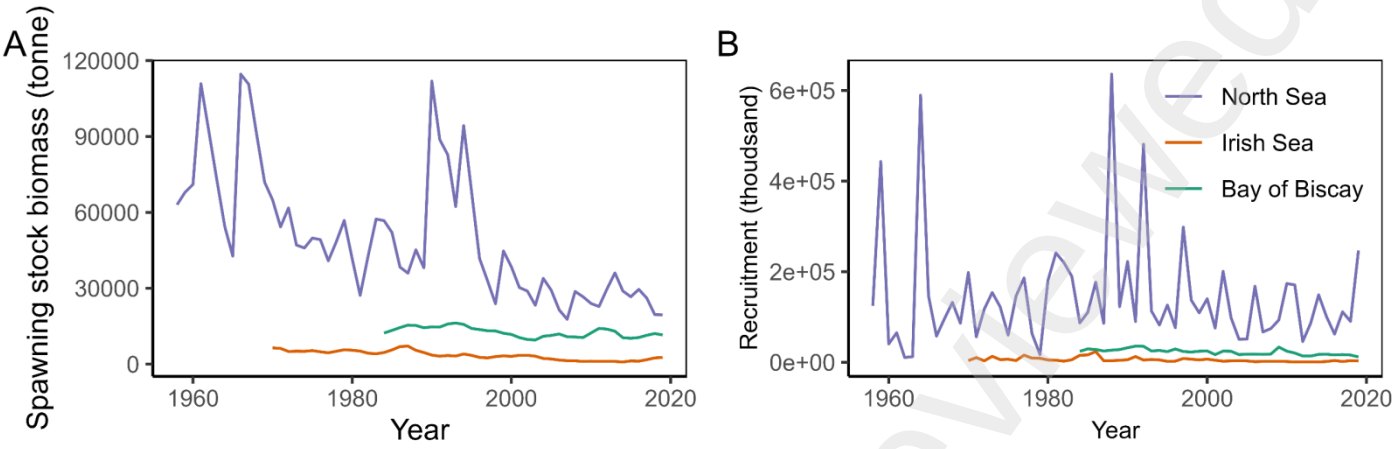

Figure S14. Temporal trend of spawning stock biomass (A) and recruitment (B).

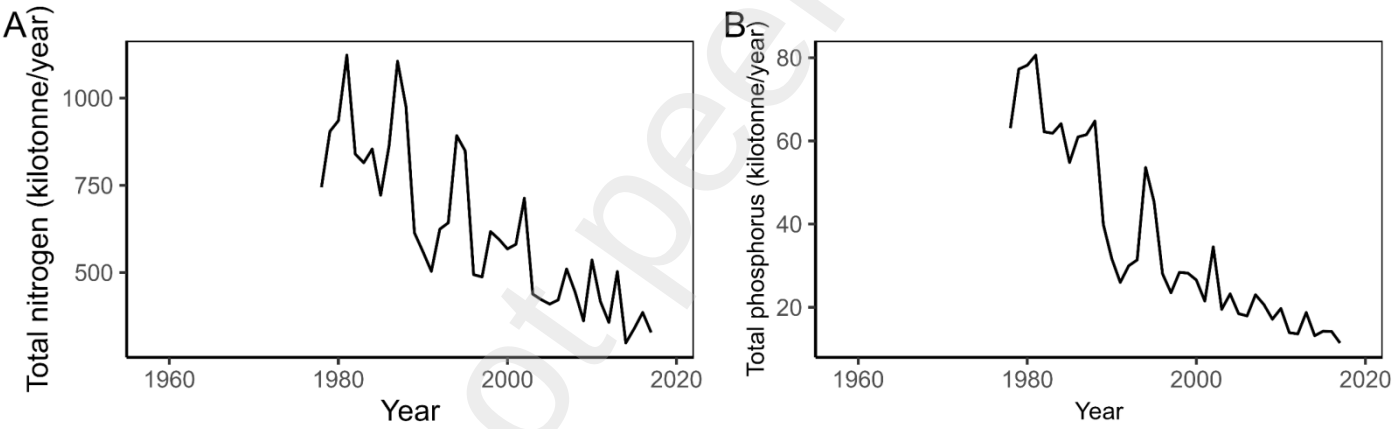

Figure S15. Temporal trend of total nitrogen (A) and total phosphorus (B) of major rivers (Rhine, Elbe, Meuse, Weser, Lake Ijssel West, Lake Ijssel East, Scheldt, Ems, and North Sea Canal) in the North Sea.

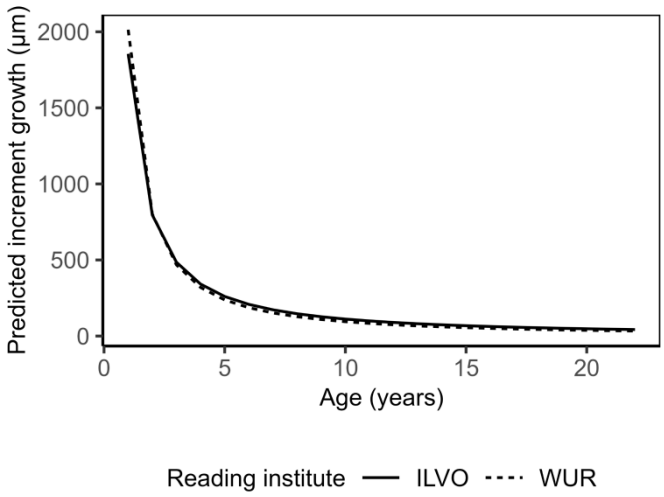

Figure S16. Predicted effect of reading institute on sole growth. 95% confidence intervals are not shown to aid clarity.

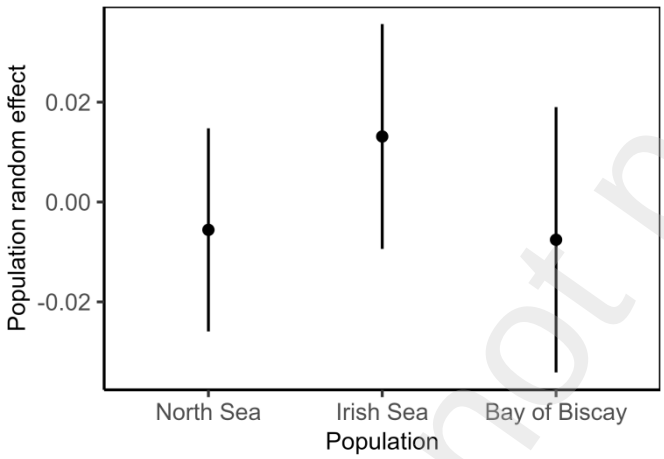

Figure S17. Population random effect. Error bars depict 95% confidence intervals.

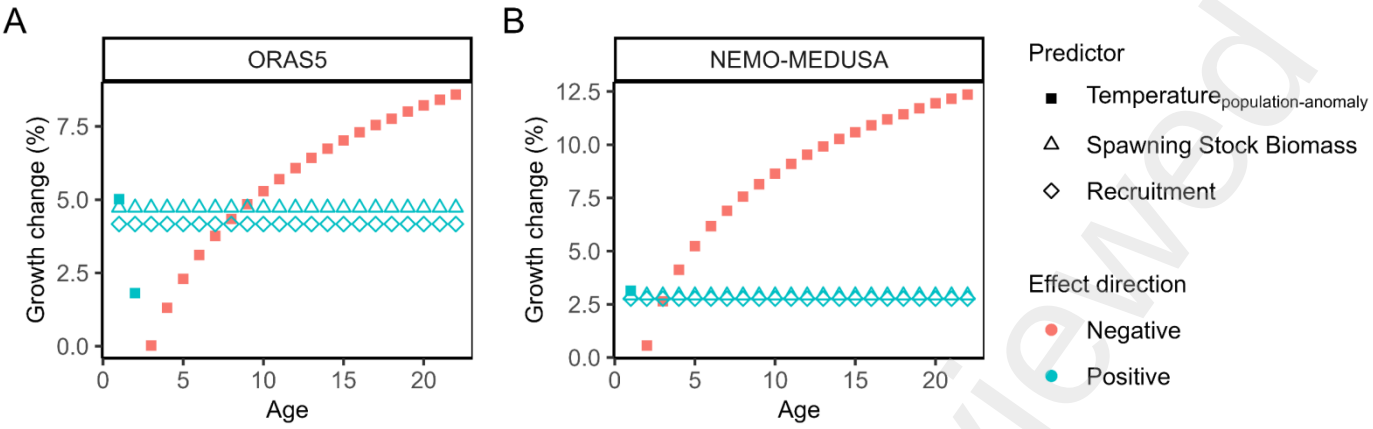

Figure S18. Predicted effects of growth predictors for each increase by one standard deviation from the best population-level extrinsic models fitted with scaled variables using ORAS5 data (A) and NEMO-MEDUSA data (B).

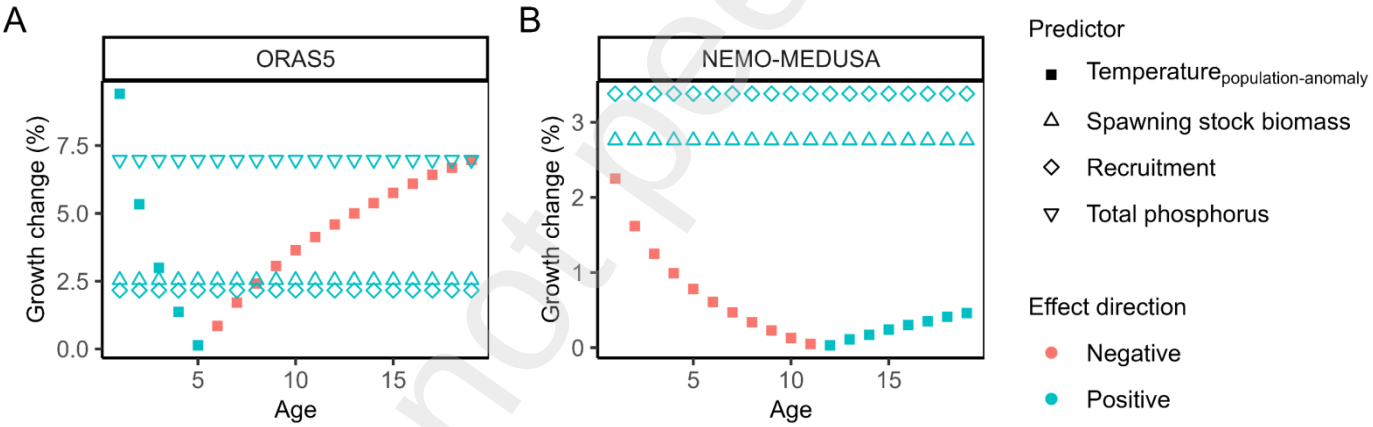

Figure S19. Predicted effects of growth predictors for each increase by one standard deviation from the best population-level extrinsic models fitted with scaled variables and nutrient data using ORAS5 data (A) and NEMO-MEDUSA data (B).

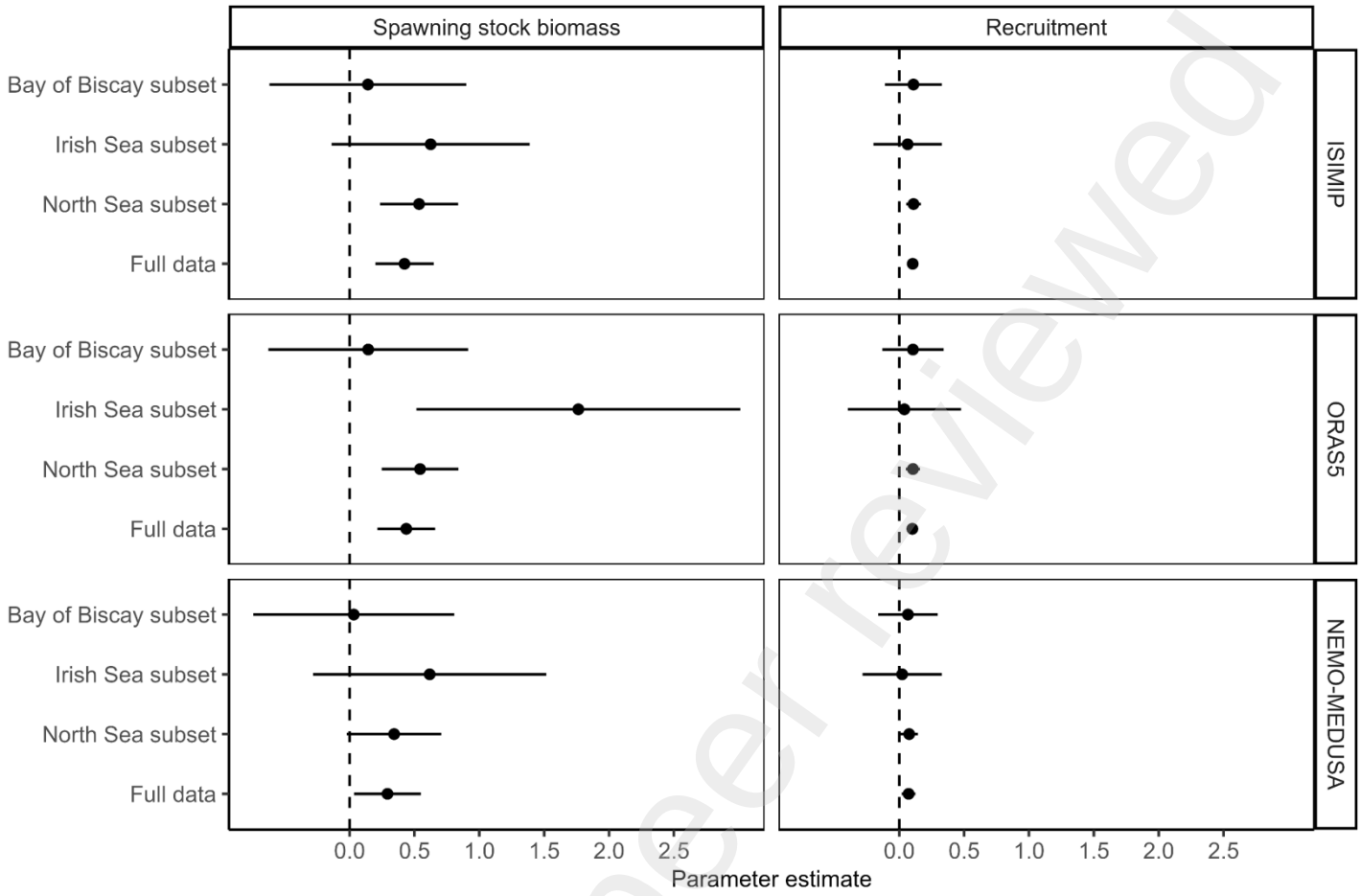

Figure S20. Parameter estimates of spawning stock biomass and recruitment effects from the best extrinsic models fitted to full data and population subset data. Error bars depict 95% confidence intervals.

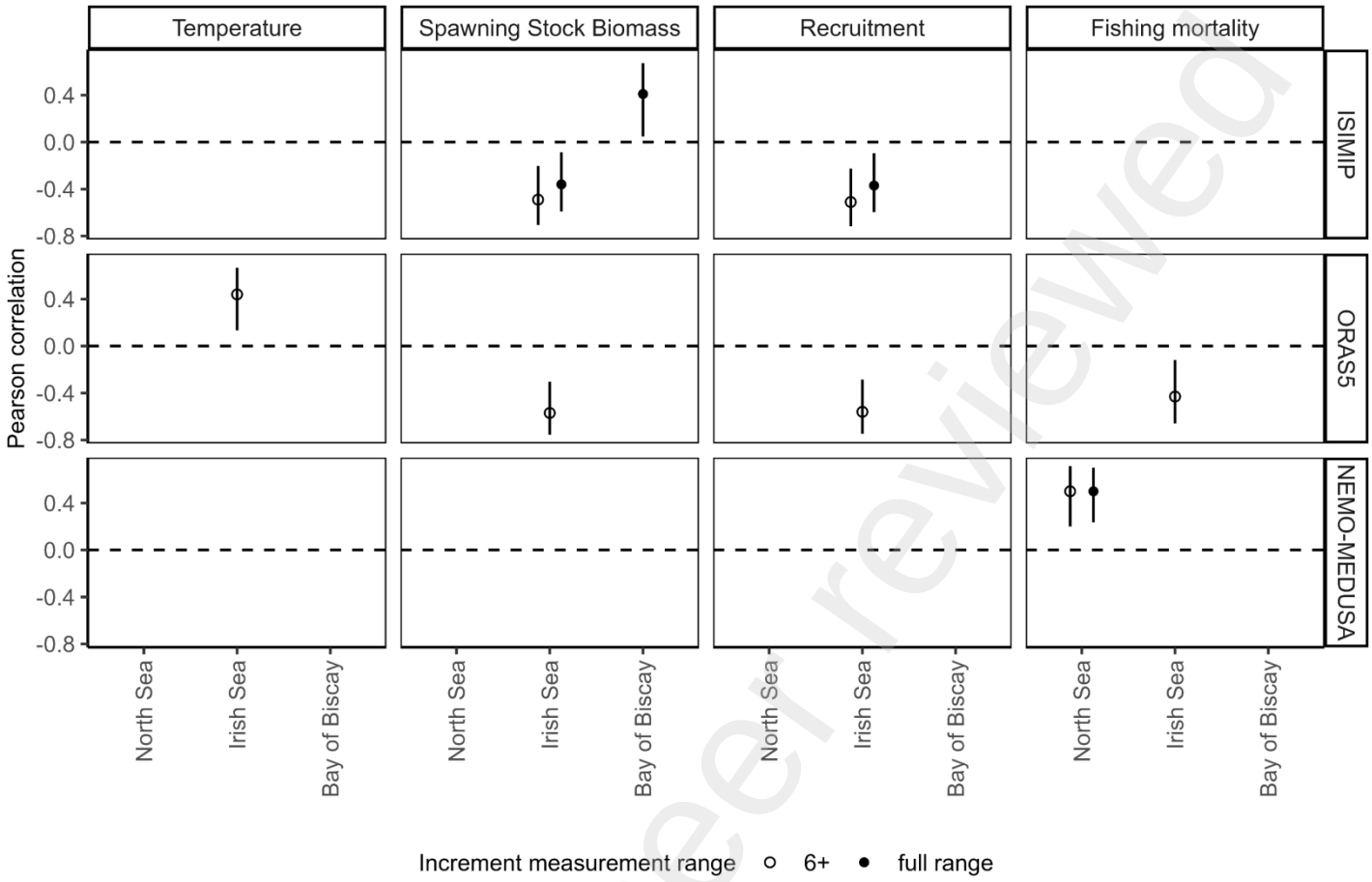

Figure S21. Pearson correlation between cohort-specific variance of individual plasticity and mean environmental conditions experienced by the cohort. Correlation test was done for two sets of increment measurement range: full range and at least six measurements. Error bars depict 95% confidence intervals.

Table S4. Selection of the best random effect structure. Series of models were fitted to the data with the maximal fixed intrinsic structure (ln(age)*preparation-method + ln(age)*reading-institute + ln(age-at-capture)). The best model is in bold. "|" indicates random age slope for a specific random term and "+" indicates that the random term was included in the model. Models with singular fit were not included in the selection.

FishID	Population	Population:Year	ln(Age)|Population:Year	Population:Cohort	ln(Age)|Population:Cohort	AICc	ΔAIC
+	**+**	**+**	**+**			**17392.74**	**0.00**
+	+	+		+	+	17475.90	83.17
+	+	+				17812.55	419.81
+	+			+		18352.72	959.99
+						18401.00	1008.26

Table S5. Selection of the best intrinsic effect structure. Series of models were fitted with the best random effect structure (**Error! Reference source not found.**). The best model is in bold. "+" indicates that the effect was included in the model. 5/18 models are presented.

Intercept	ln(Age)	ln(Age at capture)	Preparation method	Reading institute	ln(Age) * Preparation method	ln(Age) * Reading institute	AIC	ΔAIC
+	+	+	+	+		+	17330.67	0.00
+	**+**	**+**		**+**		**+**	**17331.34**	**0.67**
+	+	+	+	+	+	+	17333.22	2.55
+	+	+	+		+		17339.11	8.44
+	+	+	+	+	+		17341.10	10.43

Table S6. Selection of the best population-level extrinsic effect structure. Series of models were fitted with the best random effect structure (**Error! Reference source not found.**) and the best fixed intrinsic structure (**Error! Reference source not found.**). The best models are in bold. "+" indicates that the effect was included in the model. For each analysis using a specific temperature dataset, 5/486 models are presented. Abbreviations: SSB, spawning stock biomass; Rec, recruitment; F, fishing mortality.

SSB	**SSB * ln(Age)**	**Rec**	**Rec * ln(Age)**	**F**	**$T_{population-average}$**	**$T_{population-anomaly}$**	**$T_{population-anomaly}$ * ln(Age)**	**$T_{population-anomaly}$ * SSB**	**$T_{population-anomaly}$ * Rec**	**$T_{population-anomaly}$ * F**	**$T_{population-anomaly}$ * $T_{population-average}$**	**AICc**	**ΔAIC**	**ModelID**	**No. variable added**	**Temperature dataset**	**Year range**
+		+			+	+	+					17308.78	0.00	1	5	ISIMIP	1958 - 2019
+		+				+	+					17308.85	0.07	2	4	ISIMIP	1958 - 2019
+		+			+							17309.21	0.43	3	3	ISIMIP	1958 - 2019

+		**+**									**17309.31**	**0.53**	**4**	**2**	**ISIMIP**	**1958 - 2019**
+		+			+	+	+				+	17309.52	0.74	5	6	ISIMIP	1958 - 2019
+		+		+		+	+	+		+		17301.71	0.00	1	7	ORAS5	1958 - 2019
+		+				+	+	+				17301.77	0.07	2	5	ORAS5	1958 - 2019
+		+		+	+	+	+	+		+		17302.65	0.94	3	8	ORAS5	1958 - 2019

+		+		+		+	+	+				17302.79	1.09	4	6	ORAS5	1958 - 2019
+		**+**				**+**	**+**					**17303.39**	**1.68**	**13**	**4**	**ORAS5**	**1958 - 2019**
+		+				+	+	+	+			15114.91	0.00	1	6	NEMO-MEDUSA	1980 - 2019
+		+				+	+	+				15116.22	1.31	2	5	NEMO-MEDUSA	1980 - 2019
+		+			+	+	+	+	+			15116.42	1.51	3	7	NEMO-MEDUSA	1980 - 2019

+		+	+			+	+	+	+			15116.84	1.93	4	7	NEMO-MEDUSA	1980 - 2019
+		**+**				**+**	**+**					**15117.89**	**2.98**	**9**	**4**	**NEMO-MEDUSA**	**1980 - 2019**

Table S7. Comparison between population-level extrinsic models (from the best structures in **Error! Reference source not found.**) with and without nutrient data. Models were refitted with North Sea data in the 1978-2017 period. The best models are in bold. "+" indicates that the effect was included in the model. Abbreviations: SSB, spawning stock biomass; Rec, recruitment.

SSB	Rec	$Temperature_{population\text{-}anomaly}$	$Temperature_{population\text{-}anomaly}$ * ln(Age)	Total nitrogen	Total phosphorus	AICc	ΔAIC	Temperature dataset
+	**+**				**+**	**7853.87**	**0.00**	**ISIMIP**
+	+					7857.77	3.89	ISIMIP
+	+			+		7858.45	4.58	ISIMIP
+	**+**	**+**	**+**		**+**	**7848.44**	**0.00**	**ORAS5**
+	+	+	+	+		7855.74	7.29	ORAS5
+	+	+	+			7855.75	7.31	ORAS5
+	+	+	+		+	7652.01	0.00	NEMO-MEDUSA
+	**+**	**+**	**+**			**7653.59**	**1.59**	**NEMO-MEDUSA**

+	+	+	+	+		7654.71	2.71	NEMO-MEDUSA

Table S8. Selection of the best individual-level extrinsic effect structure. Series of models were fitted with the best random effect structure (**Error! Reference source not found.**) and the best fixed intrinsic structure (**Error! Reference source not found.**). The best models are in bold. "+" indicates that the effect was included in the model. For each analysis using a specific temperature dataset, 5/96 models are presented. Abbreviations: SSB, spawning stock biomass; Rec, recruitment; F, fishing mortality.

SSB	**Rec**	**F**	**$T_{ndividual-average}$**	**$T_{individual-average}$ * ln(Age)**	**$T_{ndividual-anomaly}$**	**$T_{individual-anomaly}$ * ln(Age)**	**$T_{individual-anomaly}$ * SSB**	**$T_{individual-anomaly}$ * Rec**	**$T_{individual-anomaly}$ * F**	**$T_{individual-anomaly}$ * $T_{individual-average}$**	**AICc**	**ΔAIC**	**ModelID**	**No. variable added**	**Temperature dataset**	**Year range**
+	+	+	+	+	+		+		+	+	17119.66	0.00	1	9	ISIMIP	1958 - 2019
+	+	+	+	+	+		+	+	+	+	17119.90	0.24	2	10	ISIMIP	1958 - 2019
+	+	+	+	+	+	+	+	+	+	+	17120.40	0.74	3	11	ISIMIP	1958 - 2019

+	+	+	+	+	+	+	+		+	+	17120.46	0.80	4	10	ISIMIP	1958 - 2019
+	**+**		**+**	**+**	**+**				**+**	**+**	**17120.50**	**0.84**	**5**	**7**	**ISIMIP**	**1958 - 2019**
+	+	+	+	+		+	+		+		17275.54	0.00	1	8	ORAS5	1958 - 2019
+	+	+	+	+		+	+	+	+		17275.86	0.33	2	9	ORAS5	1958 - 2019
+	+	+	+	+		+	+		+	+	17276.54	1.00	3	9	ORAS5	1958 - 2019
+	+	+	+	+		+	+	+	+	+	17276.95	1.41	4	10	ORAS5	1958 - 2019
+	**+**	**+**	**+**	**+**		**+**		**+**			**17277.09**	**1.55**	**5**	**7**	**ORAS5**	**1958 - 2019**
+	**+**		**+**	**+**		**+**			**+**	**+**	**14884.69**	**0.00**	**1**	**7**	**NEMO-MEDUSA**	**1980 - 2019**

+	+	+	+	+		+	+		+	+	14885.78	1.09	2	9	NEMO-MEDUSA	1980 - 2019
+	+	+	+	+		+			+	+	14885.85	1.16	3	8	NEMO-MEDUSA	1980 - 2019
+	+		+	+		+		+	+	+	14886.55	1.86	4	8	NEMO-MEDUSA	1980 - 2019
+	+		+	+	+	+			+	+	14886.62	1.93	5	8	NEMO-MEDUSA	1980 - 2019

Table S9. Comparison between individual-level extrinsic models (from the best structures in **Error! Reference source not found.**) with and without nutrient data. Models were refitted with North Sea data in the 1978-2017 period. The best models are in bold. "+" indicates that the effect was included in the model. Abbreviations: SSB, spawning stock biomass; Rec, recruitment; F, fishing mortality.

SSB	Rec	F	$T_{individual-average}$	$T_{ndividual-average}$ * ln(Age)	$T_{ndividual-anomaly}$	$T_{individual-anomaly}$ * ln(Age)	$T_{individual-anomaly}$ * SSB	$T_{ndividual-anomaly}$ * Rec	$T_{individual-anomaly}$ * F	Total nitrogen	Total phosphorus	AICc	ΔAIC	Temperature dataset
+	**+**		**+**	**+**	**+**			**+**	**+**		**+**	**7712.38**	**0.00**	**ISIMIP**
+	+		+	+	+			+	+	+		7717.83	5.45	ISIMIP
+	+		+	+	+			+	+			7722.61	10.23	ISIMIP
+	**+**	**+**	**+**	**+**			**+**	**+**			**+**	**7752.80**	**0.00**	**ORAS5**
+	+	+	+	+			+	+				7756.22	3.42	ORAS5
+	+	+	+	+			+	+		+		7756.50	3.69	ORAS5
+	+		+	+		+		+	+		+	7634.56	0.00	NEMO-MEDUSA
+	**+**		**+**	**+**		**+**		**+**	**+**			**7635.44**	**0.89**	**NEMO-MEDUSA**
+	+		+	+		+		+	+	+		7636.83	2.27	NEMO-MEDUSA

Table S10. Parameter estimates of the best intrinsic and population-level extrinsic models. Estimates are given for fixed effects with standard error (SE). Residual variance (σ^2), the variance associated with tested effects (τ) and their correlations (ρ) are given for random effects.

	Intrinsic model	**Population-level extrinsic model (ISIMIP)**	**Population-level extrinsic model (ORAS5)**	**Population-level extrinsic model (NEMO-MEDUSA)**
Fixed Effects	**Estimate (SE)**	**Estimate (SE)**	**Estimate (SE)**	**Estimate (SE)**
Intercept	7.85 (0.03)	7.74 (0.06)	7.73 (0.06)	7.82 (0.04)
ln(Age)	-1.22 (0.02)	-1.22 (0.02)	-1.22 (0.02)	-1.25 (0.02)
ln(Age at capture)	-0.15 (0.01)	-0.15 (0.01)	-0.16 (0.01)	-0.15 (0.01)
Reading Institute (WUR)	0.08 (0.03)	0.07 (0.03)	0.09 (0.03)	0.13 (0.04)
Reading Institute (WUR) * ln(Age)	-0.11 (0.02)	-0.11 (0.02)	-0.12 (0.02)	-0.14 (0.03)
Spawning stock biomass		0.42 (0.11)	0.44 (0.11)	
Recruitment		0.10 (0.02)	0.10 (0.02)	0.08 (0.03)
$T_{population\text{-}anomaly}$			0.10 (0.03)	0.05 (0.03)

$T_{population\text{-}anomaly}$ * ln(Age)			-0.09 (0.03)	-0.10 (0.03)
Random Effects				
σ^2	0.17	0.17	0.17	0.16
τ_{00}	0.01 $_{FishID}$	0.01 $_{FishID}$	0.01 $_{FishID}$	0.02 $_{FishID}$
	0.02 $_{Population:Year}$	0.02 $_{Population:Year}$	0.02 $_{Population:Year}$	0.02 $_{Population:Year}$
	0.00 $_{Population}$	0.01 $_{Population}$	0.01 $_{Population}$	0.00 $_{Population}$
τ_{11}	0.03 ln(Age)|Population:Year	0.03 ln(Age)|Population:Year	0.03 ln(Age)|Population:Year	0.02 ln(Age)|Population:Year
ρ_{01}	-0.82 $_{Population:Year\text{-}ln(Age)}$	-0.88 $_{Population:Year\text{-}ln(Age)}$	-0.88 $_{Population:Year\text{-}ln(Age)}$	-0.88 $_{Population:Year\text{-}ln(Age)}$
N	2154 $_{FishID}$	2154 $_{FishID}$	2154 $_{FishID}$	1942 $_{FishID}$
	3 $_{Population}$	3 $_{Population}$	3 $_{Population}$	3 $_{Population}$
	62 $_{Year}$	62 $_{Year}$	62 $_{Year}$	40 $_{Year}$
Observations	15260	15260	15260	13367
Marginal R^2 / Conditional R^2	0.80 / 0.85	0.81 / 0.86	0.81 / 0.86	0.82 / 0.86

Table S11. Parameter estimates of the best population-level extrinsic models with nutrient data refitted with North Sea data in the 1978-2017 period. Estimates are given for fixed effects with standard error (SE). Random effects are not presented.

	Population-level extrinsic model (ISIMIP)	**Population-level extrinsic model (ORAS5)**	**Population-level extrinsic model (NEMO-MEDUSA)**
Fixed Effects	**Estimate (SE)**	**Estimate (SE)**	**Estimate (SE)**
Spawning Stock Biomass	0.279 (0.184)	0.301 (0.174)	0.264 (0.186)
Recruitment	0.063 (0.033)	0.052 (0.032)	0.068 (0.036)
Total Phosphorus	0.002 (0.001)	0.003 (0.001)	0.002 (0.001)
$T_{population\text{-}anomaly}$		0.147 (0.049)	-0.039 (0.049)
$T_{population\text{-}anomaly}$ * ln(Age)		-0.090 (0.040)	0.020 (0.043)
N	993 $_{FishID}$	993 $_{FishID}$	981 $_{FishID}$
	40 $_{Population:Year}$	40 $_{Population:Year}$	38 $_{Population:Year}$
Observations	6783	6783	6549
Marginal R^2 / Conditional R^2	0.82 / 0.85	0.82 / 0.85	0.82 / 0.85

Table S12. Parameter estimates of the best individual-level extrinsic models with nutrient data refitted with North Sea data in the 1978-2017 period. Estimates are given for fixed effects with standard error (SE). Random effects are not presented.

	Individual-level extrinsic model (ISIMIP)	**Individual-level extrinsic model (ORAS5)**	**Individual-level extrinsic model (NEMO-MEDUSA)**
Fixed Effects	**Estimate (SE)**	**Estimate (SE)**	**Estimate (SE)**
Spawning Stock Biomass	0.156 (0.277)	0.248 (0.197)	0.289 (0.192)
Recruitment	0.098 (0.045)	0.058 (0.036)	0.058 (0.037)
Fishing mortality		-0.017 (0.219)	
Total Phosphorus	0.005 (0.001)	0.004 (0.001)	
$T_{individual\text{-}anomaly}$	-0.376 (0.090)	0.696 (0.183)	-0.073 (0.067)
$T_{individual\text{-}anomaly}$ * ln(Age)	-0.076 (0.050)	-0.268 (0.043)	-0.020 (0.051)
$T_{individual\text{-}anomaly}$ * Spawning Stock Biomass	1.735 (0.295)		
$T_{individual\text{-}anomaly}$ * Recruitment			0.082 (0.050)

$T_{individual\text{-}anomaly}$ * Fishing mortality		-0.699 (0.322)	
$T_{individual\text{-}average}$	0.037 (0.072)	0.066 (0.051)	-0.226 (0.076)
$T_{individual\text{-}average}$ * ln(Age)	0.131 (0.054)		0.201 (0.064)
N	993 $_{FishID}$	993 $_{FishID}$	981 $_{FishID}$
	40 $_{Year}$	40 $_{Year}$	38 $_{Year}$
Observations	6783	6783	6549
Marginal R^2 / Conditional R^2	0.81 / 0.86	0.81 / 0.86	0.81 / 0.85

Table S13. Predicted variance ratio of $T_{population\text{-}anomaly}$ for each population pairs (North Sea/Bay of Biscay, Irish Sea/Bay of Biscay, North Sea/Irish Sea).

Temperature dataset	Population pair	Variance ratio	95% confidence interval	p-value
ISIMIP	North Sea/Bay of Biscay	4.27	2.57 - 7.08	0.00
ISIMIP	Irish Sea/Bay of Biscay	2.23	1.34 - 3.70	0.00
ISIMIP	North Sea/Irish Sea	1.91	1.15 - 3.18	0.01
ORAS5	North Sea/Bay of Biscay	2.54	1.53 - 4.21	0.00
ORAS5	Irish Sea/Bay of Biscay	1.23	0.74 - 2.05	0.41
ORAS5	North Sea/Irish Sea	2.06	1.24 - 3.41	0.01
NEMO-MEDUSA	North Sea/Bay of Biscay	1.97	1.04 - 3.73	0.04
NEMO-MEDUSA	Irish Sea/Bay of Biscay	2.13	1.13 - 4.03	0.02
NEMO-MEDUSA	North Sea/Irish Sea	0.93	0.49 - 1.75	0.81

9 References

Amara, R., 2003. Seasonal ichthyodiversity and growth patterns of juvenile flatfish on a nursery ground in the Southern Bight of the North Sea (France). Environ. Biol. Fishes 67, 191-201.

Amara, R., Desaunay, Y., Lagardere, F., 1994. Seasonal variation in growth of larval sole Solea solea (L.) and consequences on the success of larval immigration. Netherlands Journal of Sea Research 32, 287-298.

Angilletta, M.J., Jr., Steury, T.D., Sears, M.W., 2004. Temperature, Growth Rate, and Body Size in Ectotherms: Fitting Pieces of a Life-History Puzzle1. Integr. Comp. Biol. 44, 498-509.

Arnold, T.W., 2010. Uninformative Parameters and Model Selection Using Akaike's Information Criterion. The Journal of Wildlife Management 74, 1175-1178.

Atkinson, D., 1994. Temperature and Organism Size—A Biological Law for Ectotherms? 25, 1-58.

Audzijonyte, A., Jakubavičiūtė, E., Lindmark, M., Richards, S.A., 2022. Mechanistic Temperature-Size Rule Explanation Should Reconcile Physiological and Mortality Responses to Temperature. The Biological Bulletin 243, 220-238.

Audzijonyte, A., Richards, S.A., Stuart-Smith, R.D., Pecl, G., Edgar, G.J., Barrett, N.S., Payne, N., Blanchard, J.L., 2020. Fish body sizes change with temperature but not all species shrink with warming. Nat Ecol Evol 4, 809-814.

Bartoń, K., 2022. MuMIn: Multi-Model Inference, 1.47.1 ed.

Bates, D., Machler, M., Bolker, B., Walker, S., 2015. Fitting Linear Mixed-Effects Models Using {lme4}. Journal of Statistical Software 67, 1-48.

Baudron, A.R., Brunel, T., Blanchet, M.A., Hidalgo, M., Chust, G., Brown, E.J., Kleisner, K.M., Millar, C., MacKenzie, B.R., Nikolioudakis, N., Fernandes, J.A., Fernandes, P.G., 2020. Changing fish distributions challenge the effective management of European fisheries. Ecography 43, 494-505.

Baudron, A.R., Needle, C.L., Rijnsdorp, A.D., Marshall, C.T., 2014. Warming temperatures and smaller body sizes: synchronous changes in growth of North Sea fishes. Glob Chang Biol 20, 1023-1031.

Black, B.A., Boehlert, G.W., Yoklavich, M.M., 2005. Using tree-ring crossdating techniques to validate annual growth increments in long-lived fishes. Can. J. Fish. Aquat. Sci. 62, 2277-2284.

Boëns, A., Ernande, B., Petitgas, P., Lebigre, C., 2023. Different mechanisms underpin the decline in growth of anchovies and sardines of the Bay of Biscay. Evolutionary Applications 16, 1393-1411.

Bolle, L.J., Rijnsdorp, A.D., van Neer, W., Millner, R.S., van Leeuwen, P.I., Ervynck, A., Ayers, R., Ongenae, E., 2004. Growth changes in plaice, cod, haddock and saithe in the North Sea: a comparison of (post-)medieval and present-day growth rates based on otolith measurements. J. Sea Res. 51, 313-328.

Büchner, M., 2020. ISIMIP3b ocean input data (v1.3), in: Büchner, M. (Ed.), ISIMIP Repository.

Burnham, K., Anderson, D., 2002. Model selection and multi-model inference, 2 ed. Springer New York, NY.

Campana, S.E., 2001. Accuracy, precision and quality control in age determination, including a review of the use and abuse of age validation methods. J. Fish Biol. 59, 197-242.

Campana, S.E., Smoliński, S., Black, B.A., Morrongiello, J.R., Alexandroff, S.J., Andersson, C., Bogstad, B., Butler, P.G., Denechaud, C., Frank, D.C., Geffen, A.J., Godiksen, J.A., Grønkjær, P., Hjörleifsson, E., Jónsdóttir, I.G., Meekan, M., Mette, M., Tanner, S.E., van der Sleen, P., von Leesen, G., 2022. Growth portfolios buffer climate-linked environmental change in marine systems. Ecology n/a, e3918.

Campana, S.E., Thorrold, S.R., 2001. Otoliths, increments, and elements: keys to a comprehensive understanding of fish populations? Can. J. Fish. Aquat. Sci. 58, 30-38.

Clark, T.D., Sandblom, E., Jutfelt, F., 2013. Aerobic scope measurements of fishes in an era of climate change: respirometry, relevance and recommendations. J. Exp. Biol. 216, 2771-2782.

Copernicus Climate Change Service, C.D.S., 2021. ORAS5 global ocean reanalysis monthly data from 1958 to present, Copernicus Climate Change Service (C3S) Climate Data Store (CDS).

DATRAS, I.D.o.T.S.-. 2023. in: ICES, C., Denmark (Ed.).

De Jong, G., 2005. Evolution of phenotypic plasticity: patterns of plasticity and the emergence of ecotypes. New Phytol. 166, 101-118.

Denechaud, C., Smolinski, S., Geffen, A.J., Godiksen, J.A., Campana, S.E., 2020. A century of fish growth in relation to climate change, population dynamics and exploitation. Glob Chang Biol 26, 5661-5678.

EC, 2019. Regulation (EU) 2019/1241 of the European Parliament and of the Council of 20 June 2019 on the conservation of fisheries resources and the protection of marine ecosystems through technical measures, amending Council Regulations (EC) No 1967/2006, (EC) No 1224/2009 and Regulations (EU) No 1380/2013, (EU) 2016/1139, (EU)

2018/973, (EU) 2019/472 and (EU) 2019/1022 of the European Parliament and of the Council, and repealing Council Regulations (EC) No 894/97, (EC) No 850/98, (EC) No 2549/2000, (EC) No 254/2002, (EC) No 812/2004 and (EC) No 2187/2005, Official Journal of the European Union.

Enberg, K., Jørgensen, C., Dunlop, E.S., Varpe, Ø., Boukal, D.S., Baulier, L., Eliassen, S., Heino, M., 2012. Fishing-induced evolution of growth: concepts, mechanisms and the empirical evidence. Mar. Ecol. 33, 1-25.

Engelhard, G.H., Pinnegar, J.K., Kell, L.T., Rijnsdorp, A.D., 2011. Nine decades of North Sea sole and plaice distribution. ICES J. Mar. Sci. 68, 1090-1104.

Fincham, J.I., Rijnsdorp, A.D., Engelhard, G.H., 2013. Shifts in the timing of spawning in sole linked to warming sea temperatures. J. Sea Res. 75, 69-76.

Fonds, M., 1976. The influence of temperature and salinity on growth of young sole Solea solea L.

Fonseca, V.F., Neill, W.H., Miller, J.M., Cabral, H.N., 2010. Ecophys.Fish perspectives on growth of juvenile soles, Solea solea and Solea senegalensis, in the Tagus estuary, Portugal. J. Sea Res. 64, 118-124.

Garcia-Soto, C., Cheng, L., Caesar, L., Schmidtko, S., Jewett, E.B., Cheripka, A., Rigor, I., Caballero, A., Chiba, S., Báez, J.C., Zielinski, T., Abraham, J.P., 2021. An Overview of Ocean Climate Change Indicators: Sea Surface Temperature, Ocean Heat Content, Ocean pH, Dissolved Oxygen Concentration, Arctic Sea Ice Extent, Thickness and Volume, Sea Level and Strength of the AMOC (Atlantic Meridional Overturning Circulation). Frontiers in Marine Science 8.

Ghalambor, C.K., McKay, J.K., Carroll, S.P., Reznick, D.N., 2007. Adaptive versus non-adaptive phenotypic plasticity and the potential for contemporary adaptation in new environments. Funct. Ecol. 21, 394-407.

Heino, M., Díaz Pauli, B., Dieckmann, U., 2015. Fisheries-Induced Evolution. Annual Review of Ecology, Evolution, and Systematics 46, 461-480.

Hiddink, J.G., Jennings, S., Kaiser, M.J., Queirós, A.M., Duplisea, D.E., Piet, G.J., 2006. Cumulative impacts of seabed trawl disturbance on benthic biomass, production, and species richness in different habitats. Can. J. Fish. Aquat. Sci. 63, 721-736.

Hiddink, J.G., Moranta, J., Balestrini, S., Sciberras, M., Cendrier, M., Bowyer, R., Kaiser, M.J., Sköld, M., Jonsson, P., Bastardie, F., Hinz, H., 2016. Bottom trawling affects fish condition through changes in the ratio of prey availability to density of competitors. J. Appl. Ecol. 53, 1500-1510.

Hilborn, R., Quinn, T.P., Schindler, D.E., Rogers, D.E., 2003. Biocomplexity and fisheries sustainability. Proceedings of the National Academy of Sciences 100, 6564-6568.

Hixon, M.A., Johnson, D.W., Sogard, S.M., 2014. BOFFFFs: on the importance of conserving old-growth age structure in fishery populations. ICES J. Mar. Sci. 71, 2171-2185.

ICES, 2020. Working Group on Beam Trawl Surveys, ICES Scientific Reports.

ICES, 2022. Dataset on Ocean HydroChemistry.

ICES, 2023a. Working Group for the Bay of Biscay and the Iberian Waters Ecoregion (WGBIE), ICES Scientific Reports. .

ICES, 2023b. Working Group for the Celtic Seas Ecoregion (WGCSE), ICES Scientific Reports.

ICES, 2023c. Working Group on the Assessment of Demersal Stocks in the North Sea and Skagerrak (WGNSSK), ICES Scientific Reports.

Ikpewe, I.E., Baudron, A.R., Ponchon, A., Fernandes, P.G., Pinto, R., 2021. Bigger juveniles and smaller adults: Changes in fish size correlate with warming seas. J. Appl. Ecol. 58, 847-856.

IPCC, 2021. IPCC, 2021: Climate Change 2021: The Physical Science Basis. Contribution of Working Group I to the Sixth Assessment Report of the Intergovernmental Panel on

Climate Change, Cambridge, United Kingdom and New York, NY, USA, p. 2391.

Kimura, D.K., Anderl, D.M., Goetz, B.J., 2007. Seasonal marginal growth on otoliths of seven Alaska groundfish species support the existence of annual patterns. Alaska Fish. Res. Bull 12, 243-251.

Kozłowski, J., Czarnołęski, M., Dańko, M., 2004. Can Optimal Resource Allocation Models Explain Why Ectotherms Grow Larger in Cold?1. Integr. Comp. Biol. 44, 480-493.

Kröncke, I., Reiss, H., Eggleton, J.D., Aldridge, J., Bergman, M.J.N., Cochrane, S., Craeymeersch, J.A., Degraer, S., Desroy, N., Dewarumez, J.-M., Duineveld, G.C.A., Essink, K., Hillewaert, H., Lavaleye, M.S.S., Moll, A., Nehring, S., Newell, R., Oug, E., Pohlmann, T., Rachor, E., Robertson, M., Rumohr, H., Schratzberger, M., Smith, R., Berghe, E.V., van Dalfsen, J., van Hoey, G., Vincx, M., Willems, W., Rees, H.L., 2011. Changes in North Sea macrofauna communities and species distribution between 1986 and 2000. Estuar. Coast. Shelf Sci. 94, 1-15.

Lacroix, G., Maes, G.E., Bolle, L.J., Volckaert, F.A.M., 2013. Modelling dispersal dynamics of the early life stages of a marine flatfish (Solea solea L.). J. Sea Res. 84, 13-25.

Lee, R.M., 1912. An investigation into the methods of growth determination in fishes by means of scales ICES J. Mar. Sci. s1, 3-34.
Lefrancois, C., Claireaux, G., 2003. Influence of ambient oxygenation and temperature on metabolic scope and scope for heart rate in the common sole Solea solea. Mar. Ecol. Prog. Ser. 259, 273-284.
Lescrauwaet, A.-K., Debergh, H., Vincx, M., Mees, J., 2010. Fishing in the past: Historical data on sea fisheries landings in Belgium. Mar. Policy 34, 1279-1289.
Lindmark, M., Karlsson, M., Gårdmark, A., 2023. Larger but younger fish when growth outpaces mortality in heated ecosystem. eLife 12, e82996.
Lorenzen, K., Enberg, K., 2002. Density-dependent growth as a key mechanism in the regulation of fish populations: evidence from among-population comparisons. Proceedings of the Royal Society of London. Series B: Biological Sciences 269, 49-54.
Lund, I., Steenfeldt, S.J., Herrmann, B., Pedersen, P.B., 2013. Feed intake as explanation for density related growth differences of common soleSolea solea. Aquacult. Res. 44, 367-377.
Millar, C., Large, S., Magnusson, A., Pinto, C., 2023. icesSAG: Stock Assessment Graphs Database Web Services, R package version 1.4.1 ed.
Millner, R.S., Pilling, G.M., McCully, S.R., Høie, H., 2011. Changes in the timing of otolith zone formation in North Sea cod from otolith records: an early indicator of climate-induced temperature stress? Mar. Biol. 158, 21-30.
Millner, R.S., Whiting, C.L., 1996. Long-term changes in growth and population abundance of sole in the North Sea from 1940 to the present. ICES J. Mar. Sci. 53, 1185-1195.
Mollet, F.M., 2010. Evolutionary effects of fishing and implications for sustainable management: a case study of North Sea plaice and sole. Wageningen University and Research.
Mollet, F.M., Engelhard, G.H., Vainikka, A., Laugen, A.T., Rijnsdorp, A.D., Ernande, B., 2013. Spatial variation in growth, maturation schedules and reproductive investment of female sole Solea solea in the Northeast Atlantic. J. Sea Res. 84, 109-121.
Mollet, F.M., Kraak, S.B.M., Rijnsdorp, A.D., 2007. Fisheries-induced evolutionary changes in maturation reaction norms in North Sea sole Solea solea. Mar. Ecol. Prog. Ser. 351, 189-199.
Morrongiello, J.R., Horn, P.L., C, O.M., Sutton, P.J.H., 2021. Synergistic effects of harvest and climate drive synchronous somatic growth within key New Zealand fisheries. Glob Chang Biol 27, 1470-1484.
Morrongiello, J.R., Sweetman, P.C., Thresher, R.E., 2019. Fishing constrains phenotypic responses of marine fish to climate variability. J. Anim. Ecol. 88, 1645-1656.
Morrongiello, J.R., Thresher, R.E., 2015. A statistical framework to explore ontogenetic growth variation among individuals and populations: a marine fish example. Ecol. Monogr. 85, 93-115.
Morrongiello, J.R., Thresher, R.E., Smith, D.C., 2012. Aquatic biochronologies and climate change. Nature Climate Change 2, 849-857.
Neuheimer, A.B., Grønkjær, P., 2012. Climate effects on size-at-age: growth in warming waters compensates for earlier maturity in an exploited marine fish. Global Change Biol. 18, 1812-1822.
Neuheimer, A.B., MacKenzie, B.R., Payne, M.R., 2018. Temperature-dependent adaptation allows fish to meet their food across their species' range. Science Advances 4, eaar4349.
Neuheimer, A.B., Taggart, C.T., 2010. Can changes in length-at-age and maturation timing in Scotian Shelf haddock (Melanogrammus aeglefinus) be explained by fishing? Can. J. Fish. Aquat. Sci. 67, 854-865.
Nussey, D.H., Wilson, A.J., Brommer, J.E., 2007. The evolutionary ecology of individual phenotypic plasticity in wild populations. J. Evol. Biol. 20, 831-844.
OBIS, 2023. Ocean Biodiversity Information System. Intergovernmental Oceanographic Commission of UNESCO.
Pauly, D., 2021. The gill-oxygen limitation theory (GOLT) and its critics. Science Advances 7, eabc6050.
Pauly, D., Cheung, W.W.L., 2018. Sound physiological knowledge and principles in modeling shrinking of fishes under climate change. Glob Chang Biol 24, e15-e26.
Pawson, M.G., 1995. Biogeographical identification of English Channel fish and shellfish stocks, Fisheries Research Technical Report. Lowestof, p. 72.
Perrin, N., 1995. About Berrigan and Charnov's Life-History Puzzle. Oikos 73, 137-139.
Pinsky, M.L., Eikeset, A.M., McCauley, D.J., Payne, J.L., Sunday, J.M., 2019. Greater vulnerability to warming of marine versus terrestrial ectotherms. Nature 569, 108-111.
Planque, B., Fromentin, J.-M., Cury, P., Drinkwater, K.F., Jennings, S., Perry, R.I., Kifani, S., 2010. How does fishing alter marine populations and ecosystems sensitivity to climate? J. Mar. Syst. 79, 403-417.

Poloczanska, E.S., Burrows, M.T., Brown, C.J., García Molinos, J., Halpern, B.S., Hoegh-Guldberg, O., Kappel, C.V., Moore, P.J., Richardson, A.J., Schoeman, D.S., Sydeman, W.J., 2016. Responses of Marine Organisms to Climate Change across Oceans. Frontiers in Marine Science 3.

R Core Team, 2022. R: A language and environment for statistical computing. R Foundation for Statistical Computing.

Rijnsdorp, A.D., Van Beek, F.A., 1991. Changes in growth of plaice Pleuronectes platessa L. and sole Solea solea (L.) in the North Sea. Netherlands Journal of Sea Research 27, 441-457.

Rijnsdorp, A.D., Van Beek, F.A., Flatman, S., Millner, R.M., Riley, J.D., Giret, M., De Clerck, R., 1992. Recruitment of sole stocks, Solea solea (L.), in the Northeast Atlantic. Netherlands Journal of Sea Research 29, 173-192.

Rijnsdorp, A.D., van Leeuwen, P.I., Visser, T.A.M., 1990. On the validity and precision of back-calculation of growth from otoliths of the plaice, Pleuronectes platessa L. Fisheries Research 9, 97-117.

Rijnsdorp, A.D., Vingerhoed, B., 1994. The ecological significance of geographical and seasonal differences in egg size in sole Solea solea (L.). Netherlands Journal of Sea Research 32, 255-270.

Rijnsdorp, A.D., Vingerhoed, B., 2001. Feeding of plaice Pleuronectes platessa L. and sole Solea solea (L.) in relation to the effects of bottom trawling. J. Sea Res. 45, 219-229.

Rogers, S.I., 1994. Population density and growth rate of juvenile sole Solea solea (L.). Netherlands Journal of Sea Research 32, 353-360.

RStudio Team, 2022. RStudio: Integrated Development Environment for R. RStudio, PBC.

Rutterford, L.A., Simpson, S.D., Jennings, S., Johnson, M.P., Blanchard, J.L., Schön, P.-J., Sims, D.W., Tinker, J., Genner, M.J., 2015. Future fish distributions constrained by depth in warming seas. Nature Climate Change 5, 569-573.

Schindler, D.E., Hilborn, R., Chasco, B., Boatright, C.P., Quinn, T.P., Rogers, L.A., Webster, M.S., 2010. Population diversity and the portfolio effect in an exploited species. Nature 465, 609-612.

Schram, E., Bierman, S., Teal, L.R., Haenen, O., van de Vis, H., Rijnsdorp, A.D., 2013. Thermal preference of juvenile Dover sole (Solea solea) in relation to thermal acclimation and optimal growth temperature. PLoS One 8, e61357.

Smoliński, S., Deplanque-Lasserre, J., Hjörleifsson, E., Geffen, A.J., Godiksen, J.A., Campana, S.E., 2020a. Century-long cod otolith biochronology reveals individual growth plasticity in response to temperature. Scientific Reports 10, 16708.

Smoliński, S., Morrongiello, J., van der Sleen, P., Black, B.A., Campana, S.E., 2020b. Potential sources of bias in the climate sensitivities of fish otolith biochronologies. Can. J. Fish. Aquat. Sci. 77, 1552-1563.

Stawitz, C.C., Essington, T.E., 2019. Somatic growth contributes to population variation in marine fishes. J. Anim. Ecol. 88, 315-329.

Swain, D.P., Sinclair, A.F., Mark Hanson, J., 2007. Evolutionary response to size-selective mortality in an exploited fish population. Proceedings of the Royal Society B: Biological Sciences 274, 1015-1022.

Teal, L.R., de Leeuw, J.J., van der Veer, H.W., Rijnsdorp, A.D., 2008. Effects of climate change on growth of 0-group sole and plaice. Mar. Ecol. Prog. Ser. 358, 219-230.

Tinker, J.P., Howes, E.L., 2020. The impacts of climate change on temperature (air and sea), relevant to the coastal and marine environment around the UK. MCCIP Science Review 2020, 1-30.

van de Pol, M., Wright, J., 2009. A simple method for distinguishing within- versus between-subject effects using mixed models. Anim. Behav. 77, 753-758.

van der Sleen, P., Stransky, C., Morrongiello, J.R., Haslob, H., Peharda, M., Black, B.A., Juanes, F., 2018. Otolith increments in European plaice (Pleuronectes platessa) reveal temperature and density-dependent effects on growth. ICES J. Mar. Sci. 75, 1655-1663.

van Leeuwen, S., Lenhart, H., 2021. OSPAR ICG-EMO riverine database 2020-05-01 used in 2020 workshop, in: van Leeuwen, S., Lenhart, H. (Eds.), V1 ed. NIOZ.

van Rijn, I., Buba, Y., DeLong, J., Kiflawi, M., Belmaker, J., 2017. Large but uneven reduction in fish size across species in relation to changing sea temperatures. Glob Chang Biol 23, 3667-3674.

Van Walraven, L., Mollet, F.M., Van Damme, C.J.G., Rijnsdorp, A.D., 2010. Fisheries-induced evolution in growth, maturation and reproductive investment of the sexually dimorphic North Sea plaice (Pleuronectes platessa L.). J. Sea Res. 64, 85-93.

Vaz, A.C., Scarcella, G., Pardal, M.A., Martinho, F., 2019. Water temperature gradients drive early life-history patterns of the common sole (Solea solea L.) in the Northeast Atlantic and Mediterranean. Aquat. Ecol. 53, 281-294.

Verberk, W., Atkinson, D., Hoefnagel, K.N., Hirst, A.G., Horne, C.R., Siepel, H., 2021. Shrinking body sizes in response to warming: explanations for the temperature-size rule with special emphasis on the role of oxygen. Biol. Rev. Camb. Philos. Soc. 96, 247-268.

Vinagre, C., Amara, R., Maia, A., Cabral, H.N., 2008. Latitudinal comparison of spawning season and growth of 0-group sole, Solea solea (L.). Estuar. Coast. Shelf Sci. 78, 521-528.
Vinagre, C., Maia, A., Cabral, H.N., 2007. Effect of temperature and salinity on the gastric evacuation of juvenile sole Solea solea and Solea senegalensis. J. Appl. Ichthyol. 23, 240-245.
Vitale, F., Worsøe Clausen, L., Ní Chonchúir, G., 2019. Handbook of fish age estimation protocols and validation methods. ICES Cooperative Research Reports (CRR).
von Bertalanffy, L., 1938. A quantitative theory of organic growth (inquiries on growth laws. II). Human Biology 10, 181-213.
Wang, H.Y., Shen, S.F., Chen, Y.S., Kiang, Y.K., Heino, M., 2020. Life histories determine divergent population trends for fishes under climate warming. Nat Commun 11, 4088.
Wootton, H.F., Morrongiello, J.R., Schmitt, T., Audzijonyte, A., 2022. Smaller adult fish size in warmer water is not explained by elevated metabolism. Ecol. Lett. 25, 1177-1188.
Wright, P.J., Gibb, F.M., Gibb, I.M., Millar, C.P., 2011. Reproductive investment in the North Sea haddock: temporal and spatial variation. Mar. Ecol. Prog. Ser. 432, 149-160.
Yool, A., Popova, E.E., Anderson, T.R., 2013. MEDUSA-2.0: an intermediate complexity biogeochemical model of the marine carbon cycle for climate change and ocean acidification studies. Geoscientific Model Development 6, 1767-1811.
Yool, A., Popova, E.E., Coward, A.C., 2015. Future change in ocean productivity: Is the Arctic the new Atlantic? Journal of Geophysical Research: Oceans 120, 7771-7790.